공학석사학위논문

유전영동과 마이크로포어 배열을 이용한 온칩에서의 혈장 추출

On-chip Extraction of Blood Plasma using dielectrophroresis and Micropore Array

2013 년 2 월

서울대학교 대학원

기계항공공학부

주 현 상

유전영동과 마이크로포어 배열을 이용한 온칩에서의 혈장 추출

On-chip Extraction of Blood Plasma Using Dielectrophoresis and Micropore Array

지도교수 이 정 훈

이 논문을 공학석사 학위논문으로 제출함

2013 년 2 월

서울대학교 대학원

기계항공공학부

주 현 상

주현상의 공학석사 학위논문을 인준함

2013 년 2 월

위 원 장 최 만 수 (인)

부위원장 이 정 훈 (인)

위 원 전 누 리 (인)

Abstract

On-chip Extraction of Blood Plasma Using Dielectrophoresis and Micropore Array

Hyunsang Joo

School of mechanical and aerospace engineering

The graduate school

Seoul National University

This paper presented the effectiveness of dielectrophoresis (DEP) and micropore array on the microfluidic device as part of diagnostic sensors. The optimized structure of the device and its fabrication process were reported as well. Lots of attempts were made to get higher efficiency of the experiment such as to derive maximum DEP force, to extract liquid through the pore, to decrease running time *etc*.

Dielectrophoresis and micropore array membrane, two main techniques were simultaneously but independently operated with an on-chip microfluidic platform. To generate DEP force, electrode arrays which induces non-uniform electric field was required. On a device, especially around the area where electrodes exist, there

are four membranes that each have thousands of microsized pores, which permit blood plasma to pass downward. These electrode and pore array were constructed on a silicon nitride wafer using MEMS fabrication process. This fabrication process included photolithography, reactive-ion etching (RIE), physical vapor deposition (PVD), wet etching using KOH solution *etc*. The optimized shape of electrode was decided among various samples after testing motion of particles and surface treatment was also applied on membrane area to improve throughput of pores. The microfluidic channels were attached on both sides of the device.

The experiment was progressed in the way of estimation based on theoretic equations. Micro-sized beads were also tested prior to main experiment in order to determine a more specific tendency of cells motion induced by negative DEP. It was eventually possible to extract blood plasma from a small amount of diluted whole blood only with a low voltage source for operating DEP.

Keywords: Plasma extraction, Blood separation, Dielectrophoresis, Micropore array, Microfluidics

Student number: 2011-22898

Contents

List of Figures

1. Introduction

1.1 Blood for point-of-care-testing

Since the concern for healthcare and medical check-up is rising, integrated biological systems have gradually been required. In particular, these technologies can be used to develop point-of-care (POC) diagnostics and applied in some parts of a lab-on-a-chip system [1]. The importance of POC diagnostics has received an increased attention due to some advantages such as immediacy, simplicity and non-specialty. As real-time testing becomes possible without particular place or specialized person, it can achieve an early diagnosis and eventually reduce attack rate or death rate.

There are several indicators for POC testing, but blood is the one of the most important samples because it receives information from all tissues or organs throughout the body. Whole blood is made up of 40 to 50 % cells by volume and blood plasma (Red blood cells make up approximately 95% of all cells in detail.) [2, 3]. Although each component of blood has been applied on different tests, plasma is the most widely used in diagnosis [3]. However plasma separation is a preliminary step in the preparation prior to biological analysis because accuracy or sensitivity of POC testing can be yielded well with cell-free plasma. The

conventional clinical diagnostic method is centrifugal extraction but this kind of test needs long analysis time (more than 1hour), several milliliters of whole blood sample, large space and relatively high external power. In addition, it is impossible to integrate with diagnostic part under one system, which leads to labor intensive process, thus it is not suitable for POC testing.

Component	Portion	Diameter
Erythrocyte (Red blood cell)	45%	6-8 μm
Leukocyte (White blood cell)	< 1%	10-20 μm
Thrombocyte (Platelet)	< 1%	2-3 μm
Plasma	54%	

Table 1.1 Portion and diameter of each component of blood.

Figure 1.1 The conventional clinical way for plasma extraction. This centrifugal method requires long processing time, much amount of blood sample, bulky space, relatively high external power.

1.2 Current researches about blood separation

Various techniques about blood separator have been developed in order to combine it with POC diagnostics by solving present problems. The main issues in developing this kind of system are cell manipulations such as detecting, separating, or mixing cells. Therefore many researches related with POC testing have been focused on cell handling techniques. Attempts to extract plasma on a chip were not exception. For example, blood cells were separated from diluted whole blood using capillary-driven flow based on microfluidics [2-6]. Also, blood plasma was acquired by employing microfluidic channel with cross-flow filtration [7, 8], and

exploiting the Zweifach-Fung effect, a phenomenon where small particles at crossroad of a fluidic channel tend to flow into the broader channel with fast flow rate [9, 10]. Besides these methods, similar experiment has been conducted using acoustic wave [11], magnetic field [12], *etc*. Even though these methods solved present problems, some new barriers caused by miniaturizing system size have prevented them from being useful diagnostic tools. Most devices mentioned above need external support equipment or on-chip component such as valves or tube connections. These extra parts will increase the overall dimension of a system and make complicated due to connections between each part in a device [13]. Furthermore, they cannot guarantee high plasma collect rate, thus extracted plasma could be too little to be used for diagnostics.

1.3 Dielectrophoresis and its applications

One of the effective ways to solve above problems is to adopt DEP to manipulate cells. DEP, a force of charged neutral matter caused by polarization effects in non-uniform electric field, is one of the emerging techniques because it does not require labeling and contacting process and works with low voltage. DEP

force can be generated two opposite directions. When the particle permittivity is higher than that of suspending medium, DEP force is the same direction as the gradient of electric fields and the particle move toward the region of the stronger electric field. This tendency is known as positive DEP. On the contrary, when the particle permittivity is lower than that of the medium, the direction of DEP force is the opposite direction to the electric field gradient, and the particles move toward the weaker electric field. This behavior is called negative DEP.

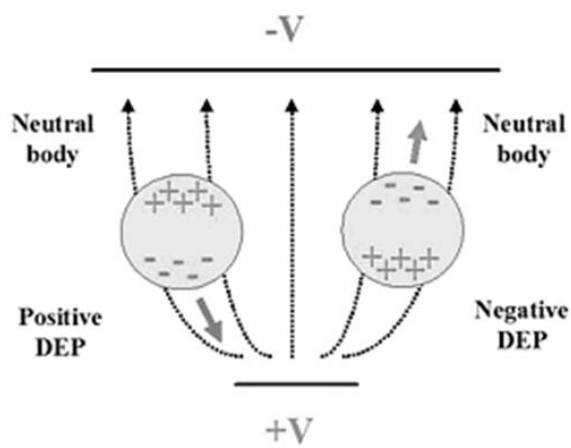

Figure 1.2 Polarization of particle in a non-uniform electric field.

This technique has applied to some kinds of cell-control device such as sorting different sized polystyrene beads, dividing between viable and non-viable yeast cells [14, 15] and separating cancer cells from blood cells [16] depending on the difference in dielectric constants or in size. However, since most of these DEP-applied researches use lateral flow in microfluidic channels, they require extra mechanical driving source like a syringe pump. Some disadvantages derived from that have been inevitable. To separate blood cells in a channel for lateral flow, cells should be forced to particular direction and thus both elongated channel length and slow flow rate are needed. It means device volume and running time become larger and longer. In addition, more blood sample should be prepared according to enlarged channel size.

In this research, we suggested new device for plasma extraction which can minimize present technical obstacles using DEP and micropore membrane. Since this device has horizontal pore membrane, separation process should be done vertically in contrast with all other present devices. This make the device be small and run in shorter time effectively. It is composed of two operating parts; electrode array for generating DEP force and micropore array for penetrating plasma, both are effective for separating blood cells. Also, we evaluated the elimination rate of blood cells and the volume ratio between before and after filtering. These two

factors were acquired with respect to various pore sizes. By comparing results of experiment, we suggested optimized device specifications.

2. Theory

2.1 DEP force expression

When a neutral particle in nonhomogeneous electric field, dipole moment is induced depending on particle size, frequency of field, dielectric properties such as conductivity, permittivity *etc*.

The DEP force F_{DEP} acting on a spherical particle immersed in a medium can be described by

$$F_{DEP} = 2\pi\epsilon_0\epsilon_m r^3 Re[f_{CM}]\,\nabla E^2 \qquad (\mathbf{2.1})$$

where r is the radius of particle, ϵ_0 is the permittivity in vacuum, ϵ_m is the relative permittivity of suspending medium, ∇E^2 is the gradient of the square of electric field and the $\mathrm{Re}[f_{CM}]$ is real part of f_{CM} called Clausius-Mossotti (CM) factor. This factor is given by

$$f_{CM} = \frac{\epsilon^*{}_p - \epsilon^*{}_m}{\epsilon^*{}_p + 2\epsilon^*{}_m} \qquad (\mathbf{2.2})$$

where $\epsilon^*{}_p$, $\epsilon^*{}_m$ are the complex permittivities of the particle and medium, respectively. It can be expressed by

$$\epsilon^* = \epsilon - j\frac{\sigma}{\omega} \qquad (\mathbf{2.3})$$

where ϵ is relative permittivity, σ is conductivity and ω is the radian frequency of electric field. The real part of CM factor determines direction of force because all other terms are always positive. If it has a plus sign, positive DEP is derived and particles are attracted. Otherwise particles are repelled by negative DEP.

2.2 DEP on blood cells

It is possible to estimate not only the magnitude but the direction of the force on each cell through the equation above. Here, we investigated the direction of blood cells with respect to frequency because the gradient and the frequency of electric field are the only things we can control without changing sample. The gradient of field, one of the two controllable things can be tuned by modification of electrode shape. However this quantity highly depends on geometric factors, thus it would be complex and hard to interpret intuitively only with theoretical analysis. This process will be discussed later. On the contrary, the frequency effect could be estimated by substituting **equation 2.3** into **equation 2.2**.

$$f_{CM} = \frac{\left(\epsilon_p - \frac{j\sigma_p}{\omega}\right) - \left(\epsilon_m - \frac{j\sigma_m}{\omega}\right)}{\left(\epsilon_p - \frac{j\sigma_p}{\omega}\right) + 2\left(\epsilon_m - \frac{j\sigma_m}{\omega}\right)}$$

$$= \frac{(\epsilon_p - \epsilon_m)(\epsilon_p + 2\epsilon_m)\omega^2 + 3(\epsilon_p\sigma_m - \epsilon_m\sigma_p)\omega j + (\sigma_p - \sigma_m)(\sigma_p + 2\sigma_m)}{(\epsilon_p + 2\epsilon_m)^2\omega^2 + (\sigma_p + 2\sigma_m)^2}$$

$$(\mathbf{2.4})$$

Since the effective term of this equation is just real part, **equation 2.4** can be simplified.

$$Re[f_{CM}] = \frac{(\epsilon_p - \epsilon_m)(\epsilon_p + 2\epsilon_m)\omega^2 + (\sigma_p - \sigma_m)(\sigma_p + 2\sigma_m)}{(\epsilon_p + 2\epsilon_m)^2\omega^2 + (\sigma_p + 2\sigma_m)^2} \qquad (\mathbf{2.5})$$

The range of the CM factor is placed on $-0.5 \leq f_{CM} \leq 1.0$ by the **equation 2.5**, thus the magnitude of the CM factor is limited even when $\epsilon^*_p \to \infty$ or $\epsilon^*_m \to \infty$. Therefore it was possible to draw the magnitude of real part of CM factor with respect to electric field frequency using **equation 2.5**. **Figure 2.1** is the result, which informs us of the DEP direction. We calculated it by substituting relative permittivity and conductivity of diluted plasma (80, 55mS/m) and those of a blood cell (63, 1μS/m) into the equation, separately [13]. The CM factor is always negative value over a frequency range shown. The maximum absolute value of the factor is 0.5 while frequency is below 1 MHz and it goes down with higher frequency. It was very important as advance information, because we did not have

to deliberate about attractive force induced by positive DEP. Therefore, we designed electrode shapes, considering only negative DEP and used relatively low frequency.

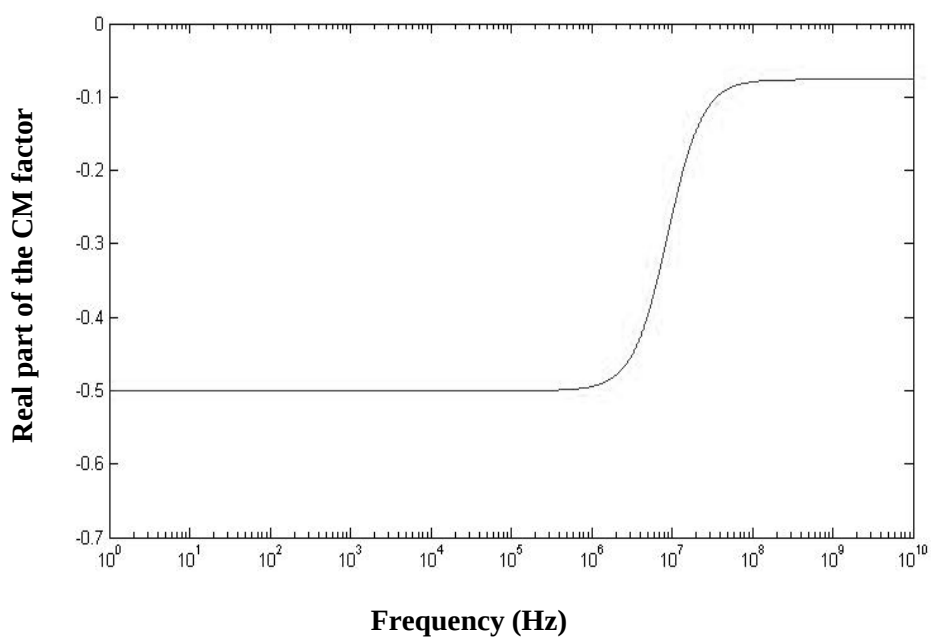

Figure 2.1 Real part of the CM factor change depending on electric field frequency.

2.3 Hydrodynamic drag force and particle velocity

If there is no DEP force, most particles could be sucked into vortex caused by pores and then get stuck. In order to prevent pore blocking, DEP force has to exceed drag force at the least. In general, hydrodynamic drag force F_{Drag} on a spherical particle is expressed by

$$F_{Drag} = -6\pi\mu r u \qquad (\mathbf{2.6})$$

where μ is fluid viscosity, r is the radius of particle and u is fluid velocity. However, if particle starts to move inside fluid, this velocity is changed to relative velocity of the particle to fluid flow, $u_{r,p}$.

$$u_{r,p} = u_{fluid} + u_{DEP} \qquad (\mathbf{2.7})$$

Here, u_{fluid} is fluid velocity and u_{DEP} is velocity induced to a particle by DEP force and these two forces are activated toward opposite direction. We can derive the equation of particle velocity by comparing DEP force and viscous drag.

$$F_{DEP} + F_{Drag} = 0 \qquad (\mathbf{2.8})$$

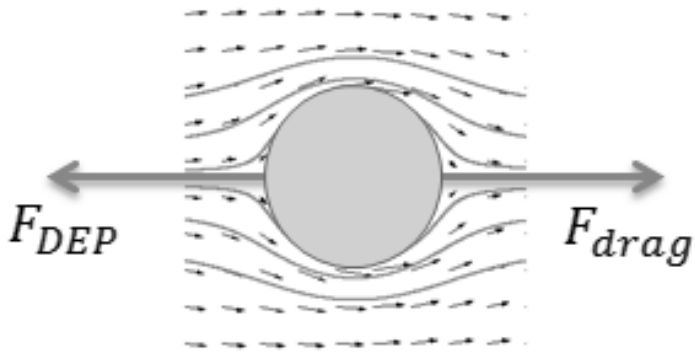

Figure 2.2 Schematic diagram of force balance between DEP force and hydrodynamic viscous force.

Comparing **equations 2.1** and **2.6** yields;

$$2\pi\epsilon_0\epsilon_m r^3 Re[f_{CM}]\,\nabla E^2 = 6\pi\mu r\left(u_{fluid} + u_{DEP}\right) \qquad (\mathbf{2.9})$$

Then, the minimum value of u_{DEP} should take the following form.

$$u_{DEP} = \frac{\epsilon_0\epsilon_m r^2}{3\mu} Re[f_{CM}]\,\nabla E^2 - u_{fluid} \qquad (\mathbf{2.10})$$

In this equation, $Re[f_{CM}]$, ∇E^2 and u_{fluid} can be tuned without changing materials, but all other terms are not changeable. The CM factor was easily fixed according to Fig 1. Since electric field gradient is highly dependent on electrode shape, we tried to obtain the optimized one by testing various shapes of electrode

with micro-polystyrene beads. In addition, fluid velocity is proportional to the diameter of pore. We also found proper flow rate adjusting pore size to increase DEP effect.

3. Materials and Methods

3.1 Working process

Since the main role of this device is on-chip blood separation, the idea at first was that whole blood would be dropped right onto electrode array as shown in **Figure 3.1**. However this method did not have high efficiency due to the distance between cells and electrodes. Since the radius of blood droplet was too long to transmit DEP force, we installed fluidic channel whose height was 50 μm on the device.

As soon as blood sample is dropped onto inlet and it is spread out all over the channel. The initial separation is started by DEP and secondary process is followed by pore membrane. While DEP force levitates blood cells, plasma can pass through pores without blocking problem. This process is shown in **Figure 3.2**. As a result of this mechanism, it is possible to operate not horizontally but vertically, unlike other conventional methods which use lateral flow. We demonstrated that this technique successfully extracted a proper amount of plasma enough to be used in POC diagnostics from a little blood sample for a short time.

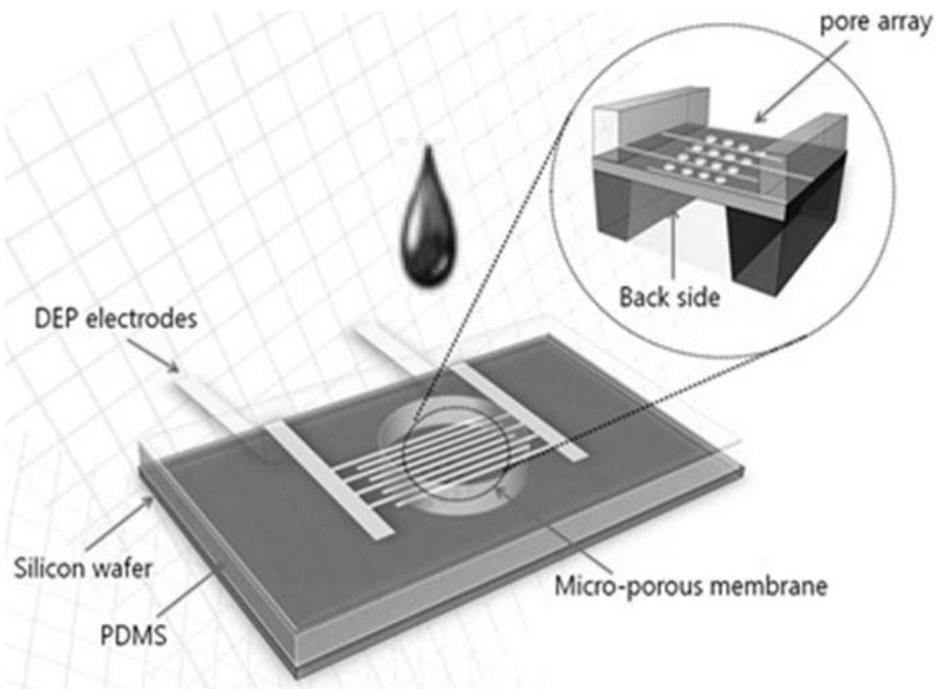

Figure 3.1 Concept image of the proposed device.

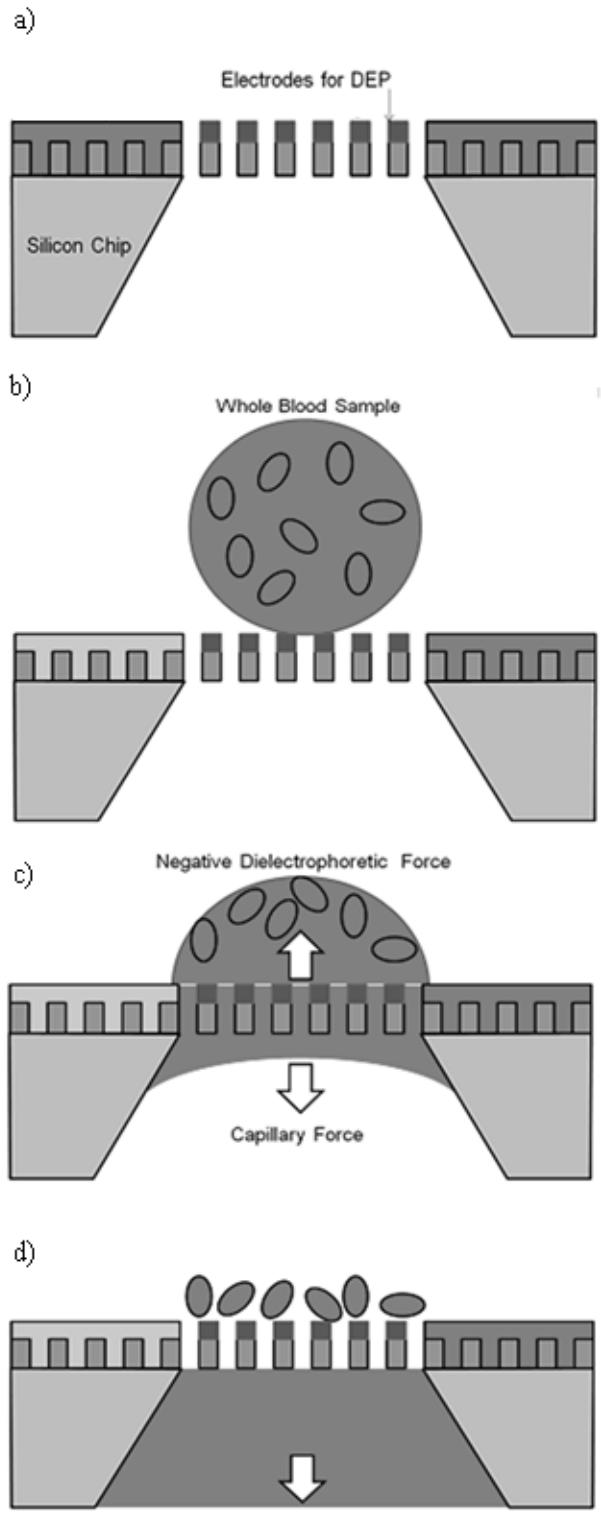

Figure 3.2 Working process of the device.

3.2 Device design

Figure 3.3 is a side view of the integrated device. As mentioned above, to use microfluidic channel was inevitable in order to make the height of blood sample maintain microscale. There is an upper channel on the chip which contains pores and electrodes for DEP. A Lower channel is also attached under the chip to be a reservoir for filtered blood. Each channel has air venting hole so that channel can be filled with fluid.

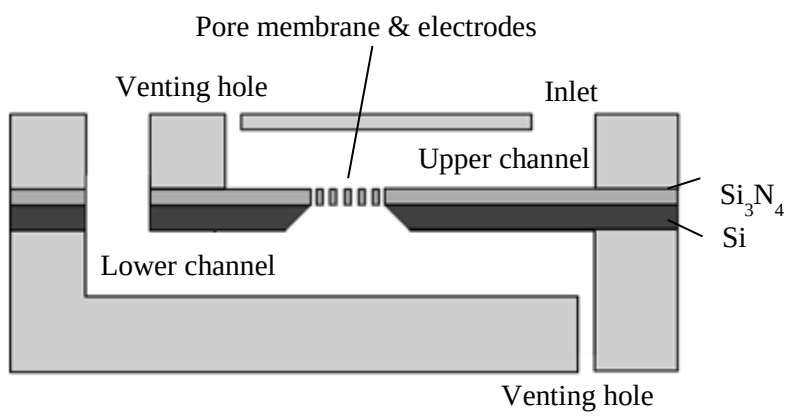

Figure 3.3 Side view of the integrated device.

3.3 Experimental outline

In the device, DEP force can filter blood cells with assistance from pore-array membrane. These tools were fabricated on a chip, then eventually microfluidic channels were attached on both sides of the chip. The frequency of the field was already decided by theoretical prediction as mentioned. Arrangement, shape and dimension of electrodes were determined by results of the pretest with microsized polystyrene beads whose diameters were 2 μm, 6 μm, 9 μm similar to the average size of different blood cell types. Only electrode array was required when we conducted this test. (Micropores did not need to be involved in the test at that moment.) Therefore we fabricated with Indium Tin Oxide (ITO) electrode on a glass wafer instead of gold electrode on a silicon nitride wafer so that we could use an inverted microscope; in general, it is useful for observing living cells or organisms under more natural conditions and used in application of micromanipulation as well. We tested diverse shapes of electrodes with an ITO-glass wafer and picked out the devices of good performance. After confirming the tendency of particle motion, we realized same pattern onto silicon nitride wafer with small change in the dimensions. Micropores, meanwhile, were tested with silicon nitride wafer to get the proper diameter of pores. We compared the results with various pore sizes from 3 μm to 15 μm, and finally decided the optimized one.

3.4 Device fabrication

3.4.1 ITO-glass wafer

The fabrication was started with ITO-deposited glass wafer. The thickness of an ITO layer was 2,000 Å. A conventional photolithography process was applied on the wafer, which was covered with a photoresist (PR) AZ 5214-E by spin-coating. After soft baking at 90 ℃ for 90 sec, it was exposed to the light by MA-6 Aligner (Karl-Suss, Germany). Electrode patterns came into the sight as the wafer soaked into a mixture of AZ 300 and deionized water (DIW) (6:1, v/v) for approximately 80 sec. Hard baking was conducted at 110 ℃ for 3 min. The ITO layer could be etched in ITO etchant, mixture of HCl, H_2O and HNO_3 (4:2:1, v/v) for about 20 sec. All remaining PR layer was removed by AZ 700 developer with sonication for 5 min. This process was presented in **Figure 3.4**

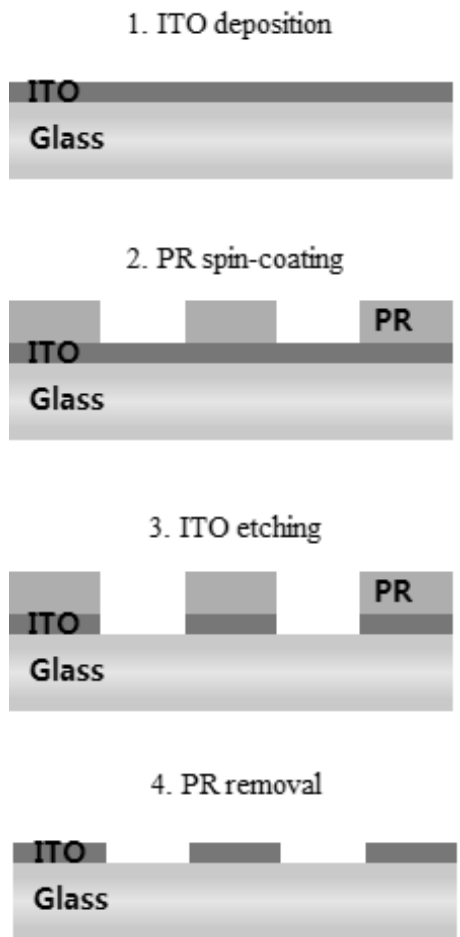

Figure 3.4 Fabrication process for ITO-glass wafer.

3.4.2 Silicon nitride wafer

Figure 3.3 briefly shows the fabrication sequence of the device. This process started with a four-inch silicon nitride wafer. A PR AZ 5214-E was spin-coated, exposed to UV light and patterned with AZ-300 solution. Subsequently, the disclosed area of silicon nitride layer passed away by dry etching using P-5000 Etcher (Applied Materials, USA). Then, a gold layer (1000 Å thick) was deposited after deposition of a thin chrome layer (200 Å thick) using e-gun evaporator (Maestech, Korea) after a negative PR DNR-L300 patterning. Lift-off process was accomplished by removing PR. This removing process required acetone with sonication. Then, a silicon nitride layer on the back side was partially eliminated after bottom side alignment using PR AZ-5214-E so that KOH solution could reach silicon surface. A silicon wafer (500 μm thick) was etched by KOH solution (40%, w/v) for approximately 12 hours at 70 ℃ (etch rate was about 0.73 μm/min). Since this etching process is anisotropic, sidewalls formed a 54.7° angle with the horizontal surface. Oxygen plasma treatment was applied on both sides of silicon nitride surface to make it hydrophilic using Plasmalab 80 plus (Oxford instrument, England).

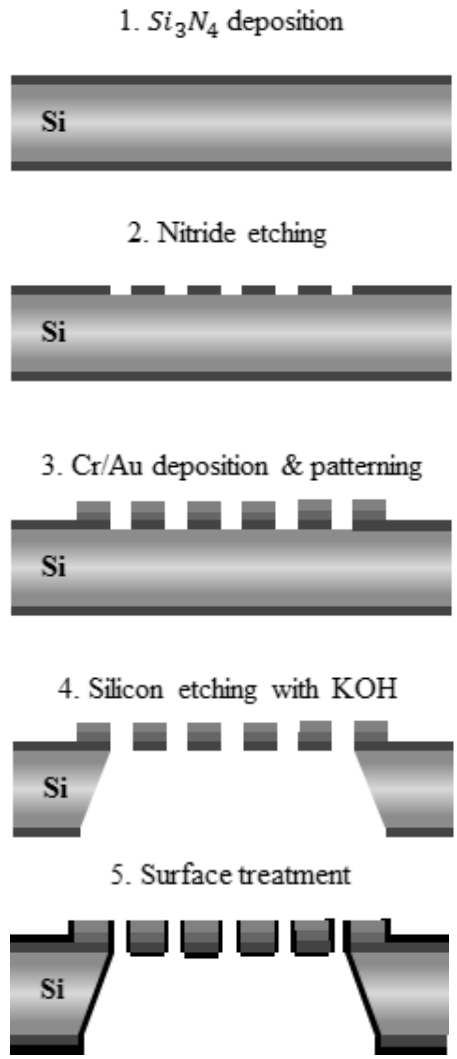

Figure 3.5 Fabrication sequences of electrodes and pores on a silicon nitride wafer.

3.4.3 Microfluidic channel

Microfluidic cannels, on the other hand, were produced by molding process. To increase adhesion, a silicon wafer was treated by PVA Tepla microwave asher (PVA Tepla AG, Germany). A PR Su-8 3050 was spin-coated (500 rpm, 5 sec and then 3000 rpm, 35 sec) onto silicon wafer with a thickness of 50 μm and baked at 95 ℃ for 35 min. After exposure, it required post exposure baking (PEB) at 65 ℃ for 1 min and then at 95 ℃ for 5 min. A Su-8 developer removed the exposed area for about 8 min and the wafer should be soaked into DIW and Isopropyl alcohol (IPA) by turns. This fabrication was completed by hard baking (at 180 ℃ for 5 min).

The fabricated wafer was used as a mold. A mixture of polydimethlysiloxane (PDMS) and a curing agent (10:1, w/w) was poured onto the mold and degassed. Then, it was baked in an oven at 70 ℃ for more than 2 hours. The cured PDMS mixture got stripped off from the mold and punched to form an inlet and air-venting holes. We attached two slices on each side of the device using high-frequency generator (Electro-Technic Products, USA). All these steps can be summarized as **Figure 3.6**. **Figure 3.7** shows the completed PDMS channels with blue ink to make its boundary easy to recognize.

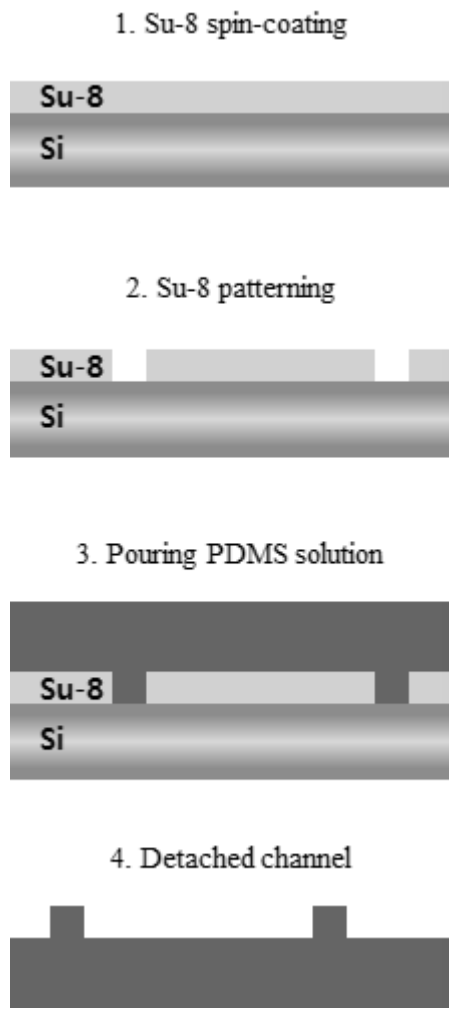

Figure 3.6 Fabrication steps for making PDMS microfluidic channel.

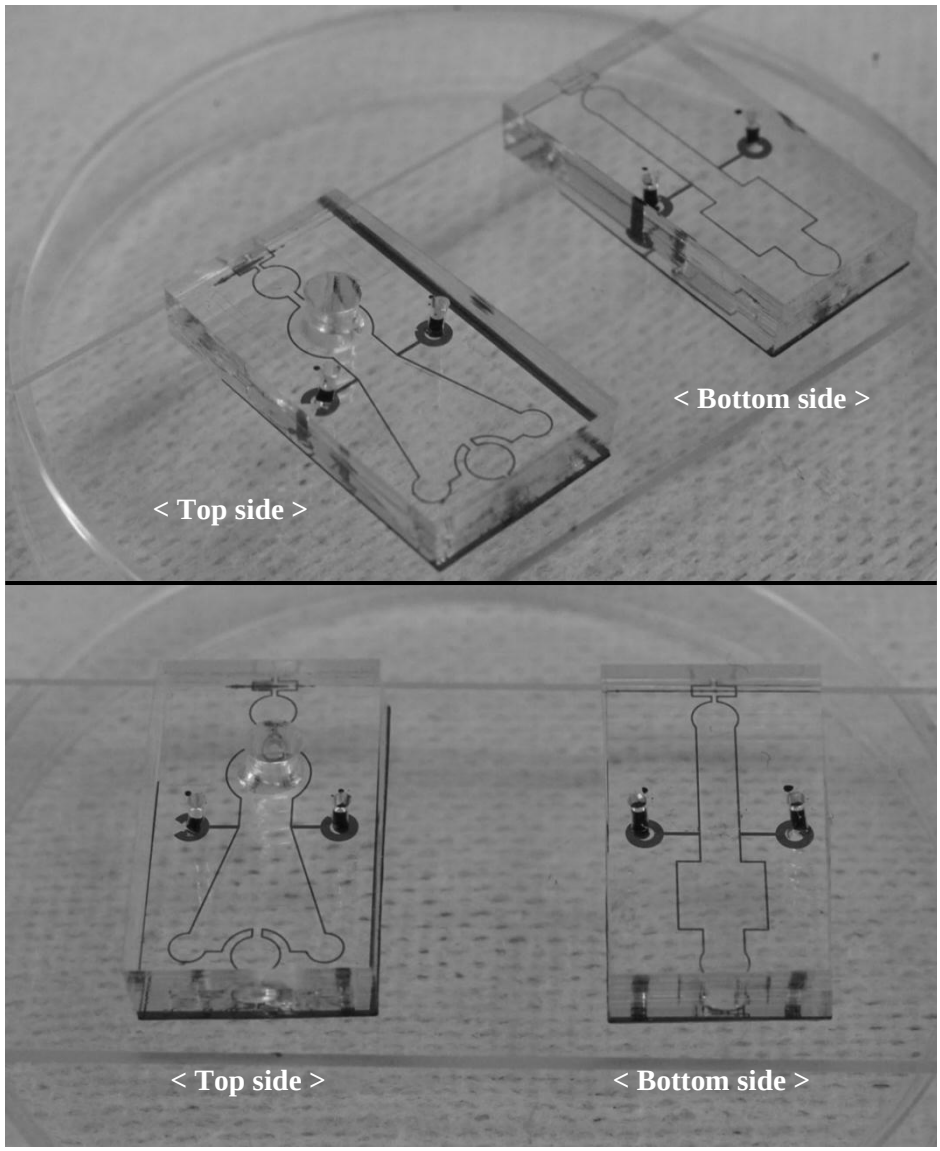

Figure 3.7 Two kinds of microfluidic channel.

Figure 3.8 is a photograph of the integrated device and **Figure 3.9** is a magnified image taken by scanning electron microscope (SEM). There are small holes between every electrode.

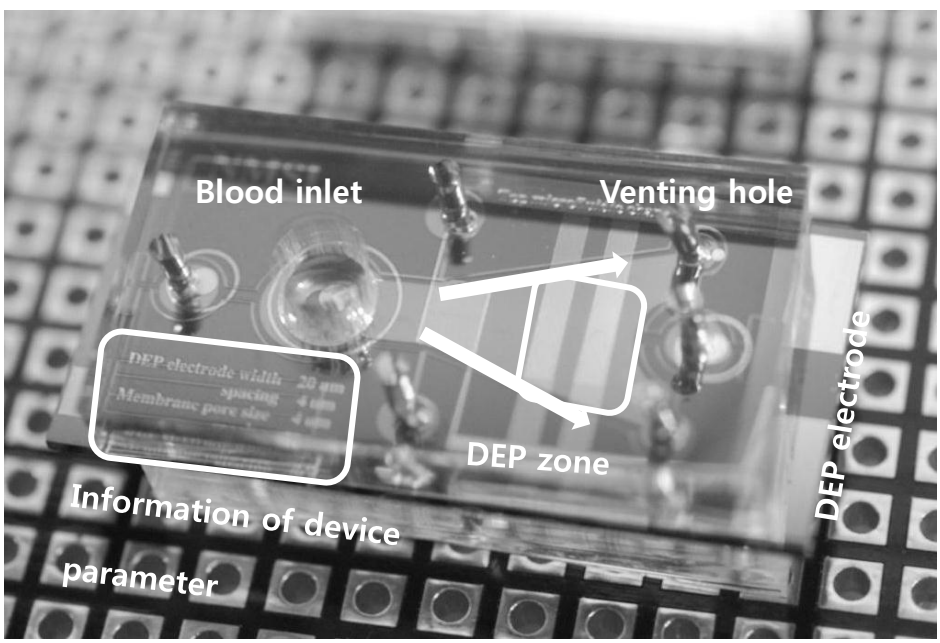

Figure 3.8 The integrated device.

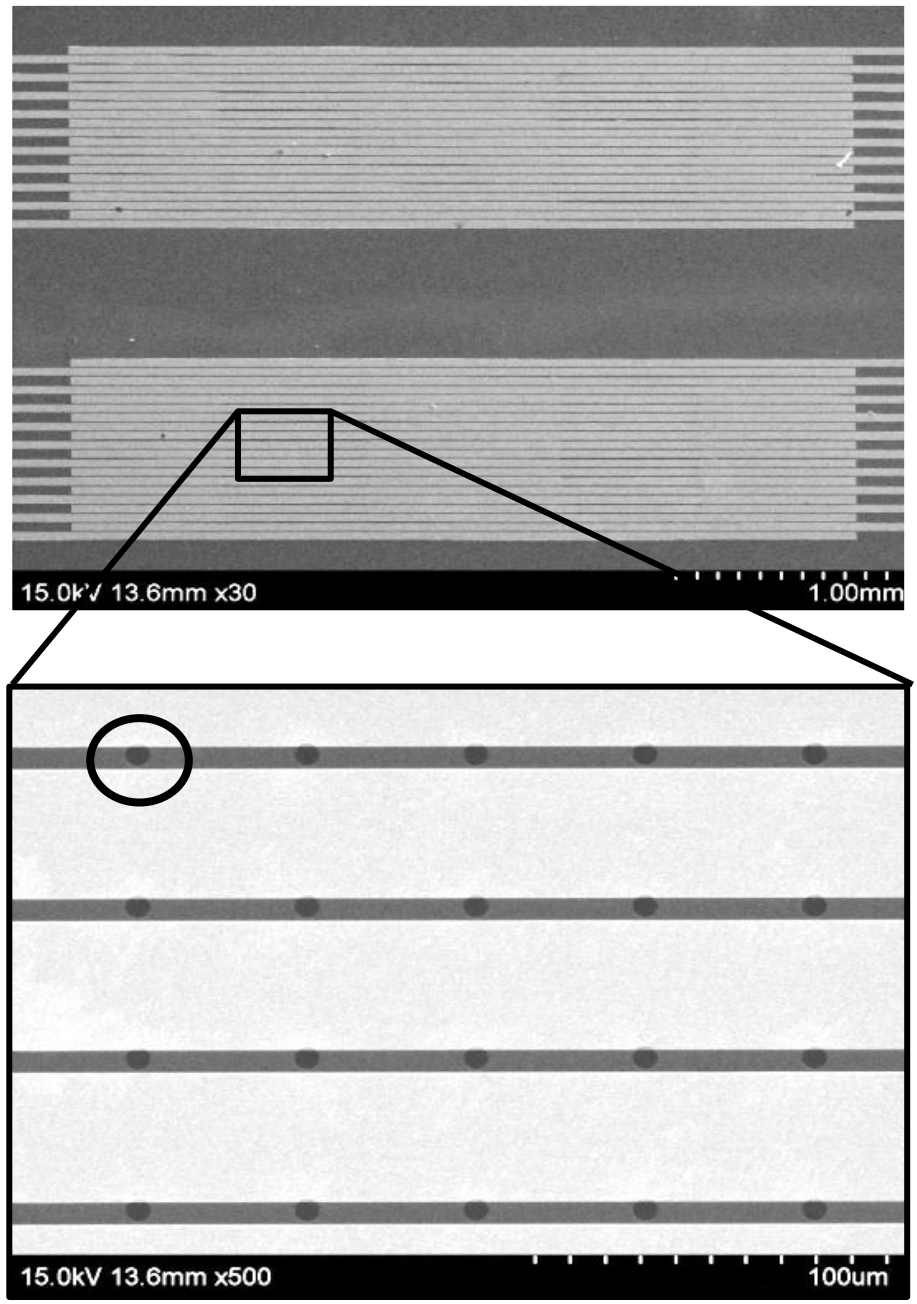

Figure 3.9 SEM images of electrodes and pore array.

3.5 Experimental setup

We plastered inner walls of channels with 1% (w/w) bovine serum albumin (BSA) (Biosesang, Korea) solution which interrupts cells adhesion on the wall, before combining the device and microfluidic channels. Also, channels were treated by high-frequency generator so that blood might diffuse fast owing to hydrophilic surface. Otherwise, flow would be stopped since PDMS is naturally hydrophobic material. A function generator (Tektronix, USA) was used to generate alternating current (AC). It connected to pads on the device through needle electrodes. Since the device operated along vertical direction, we captured data using microscopes from various angle to get precise figures. Three different types of the devices were used for observation. An inverted microscope was helpful in watching the motion of particles with ITO electrode on glass wafer (**Figure 3.10**). Movement on a silicon wafer was observed by a metal microscope (**Figure 3.11**). A macroscopic camera enabled us to measure a change in volume of blood droplet (**Figure 3.12**).

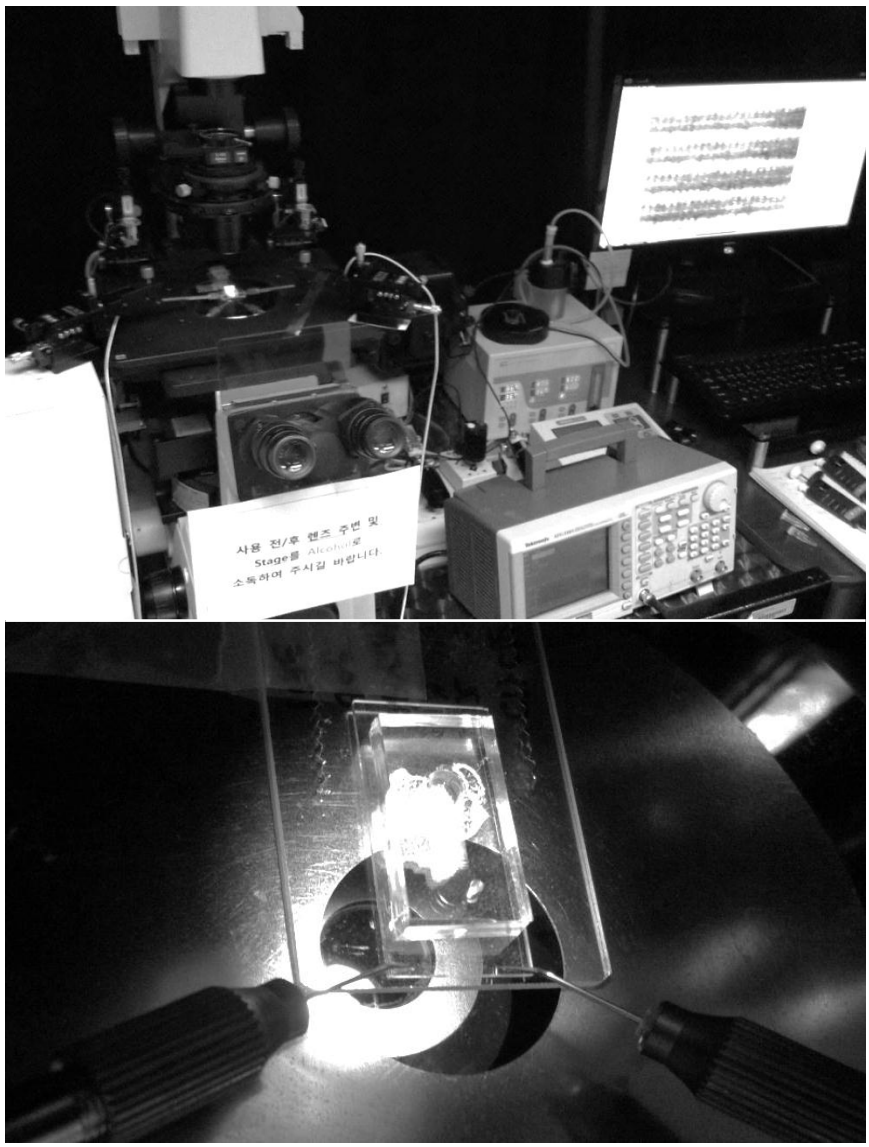

Figure 3.10 Experimental setup with an inverted microscope.

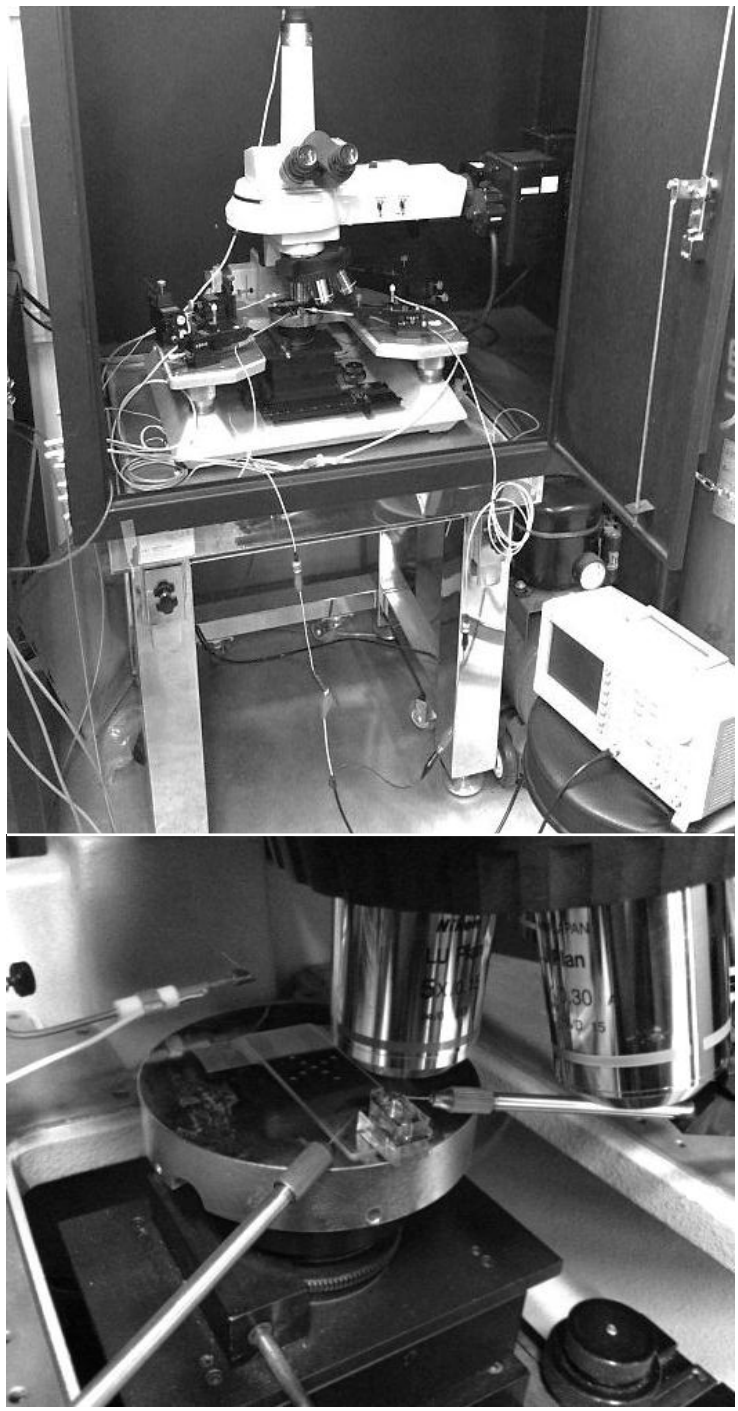

Figure 3.11 Experimental setup with a metal microscope.

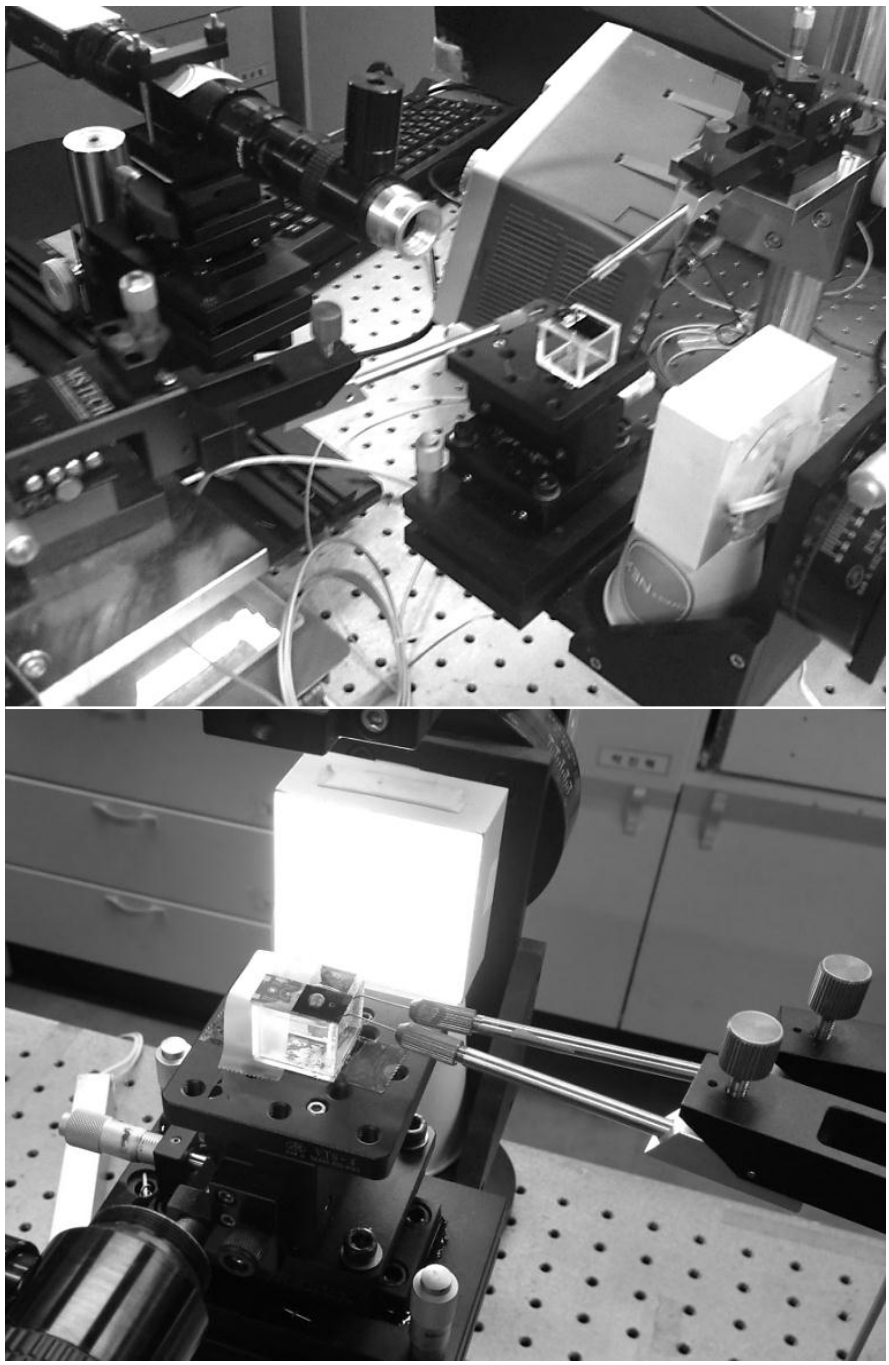

Figure 3.12 Experimental setup with a macroscopic camera.

3.6 Sample preparation

Whole blood was drawn from healthy adult donor through venipuncture. An ethylenediaminetetraacetic acid (EDTA) vacutainer tube was used as storage without coagulation. Whole blood was diluted with isotonic buffer with different concentrations. This buffer was made up of 8.5% (w/v) sucrose and 0.3% (w/v) dextrose in 1X phosphate buffered saline (PBS). BSA powder was also added into the solution with concentration 1% (w/w). Approximately 20 µL of diluted blood was dropped into the inlet at a time.

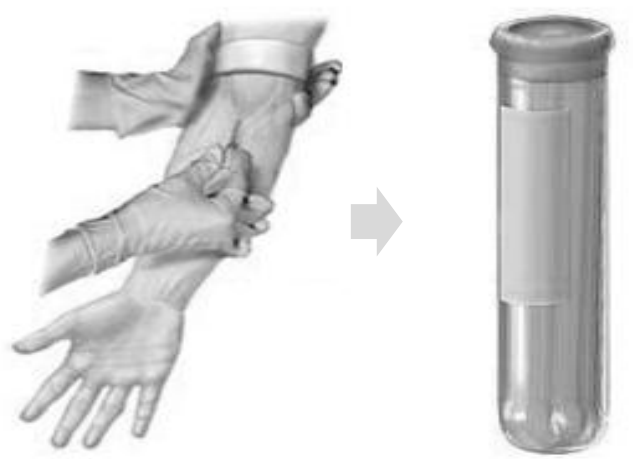

Figure 3.13 Blood extraction through venipuncture and EDTA tube.

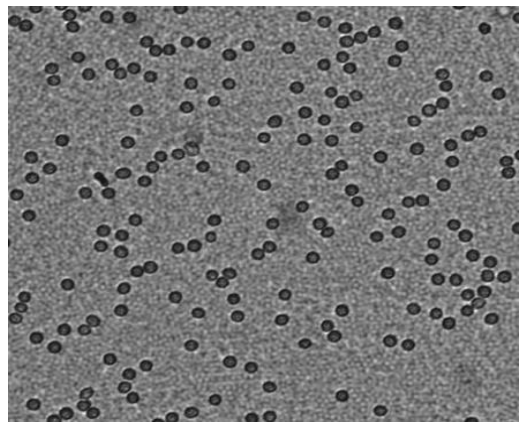

(1:100)

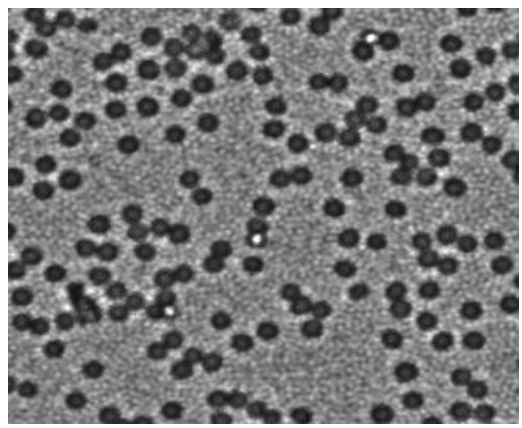

(1:40)

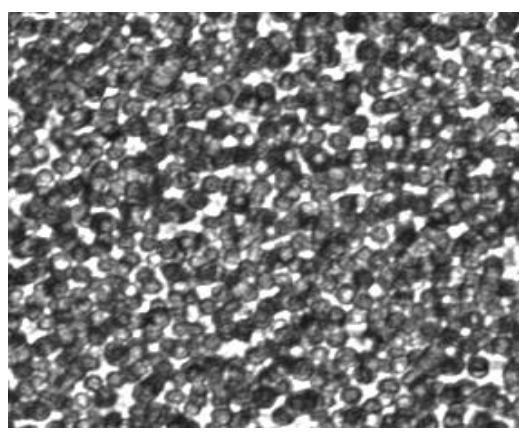

(1:10)

Figure 3.14 Microscope images of red blood cells in different concentrations.

3.7 Evaluation methods

In order to judge device performance objectively, we reported each experimental data and derived two indicators from them. The first one is the purity which means blood cells removal efficiency from whole blood. The other one is the plasma recovery defined as the percentage of the filtered output volume compared to the amount of input. It is directly proportional to flow rate through the pores. Prior to calculating these two factors, we figured out where DEP force was maximized in terms of voltage and frequency. After measuring and comparing the results with respect to pore size, it was possible to find the most appropriate dimensions.

4. Results and Discussion

4.1 Pretest with microbeads

Experiments with microbeads were conducted to predict magnitude of DEP force depending on electrode shape, before dealing with red blood cells. Since many shapes could be drawn on a photolithographic mask, some different sorts were produced by one-cycle fabrication process. **Figure 4.1** shows some representative types of many shapes. We carried out test with 0.5% w/v polystyrene microbeads without any function group. About 20 μL of bead solution was injected to device via inlet. We waited until channel was totally filled with solution. When motion of fluid was negligible, AC electric field was applied using a function generator. As presented in **Figure 4.2**, it was impossible to figure out electrode array due to lots of beads, but almost all of them were swept away from the intended area and electrode shape became notable. Here, the intended area meant the region where we expected that beads were under repulsion force, in general, the place keeping short distance between electrode pair. **Figure 4.2 (b), (c), (d), (e)** are some examples which represented particles movement well. The working voltage was higher than 5 Vpp (offset: 0 V) and AC frequency was around 100 kHz (sine wave). These processes were done within 2 min.

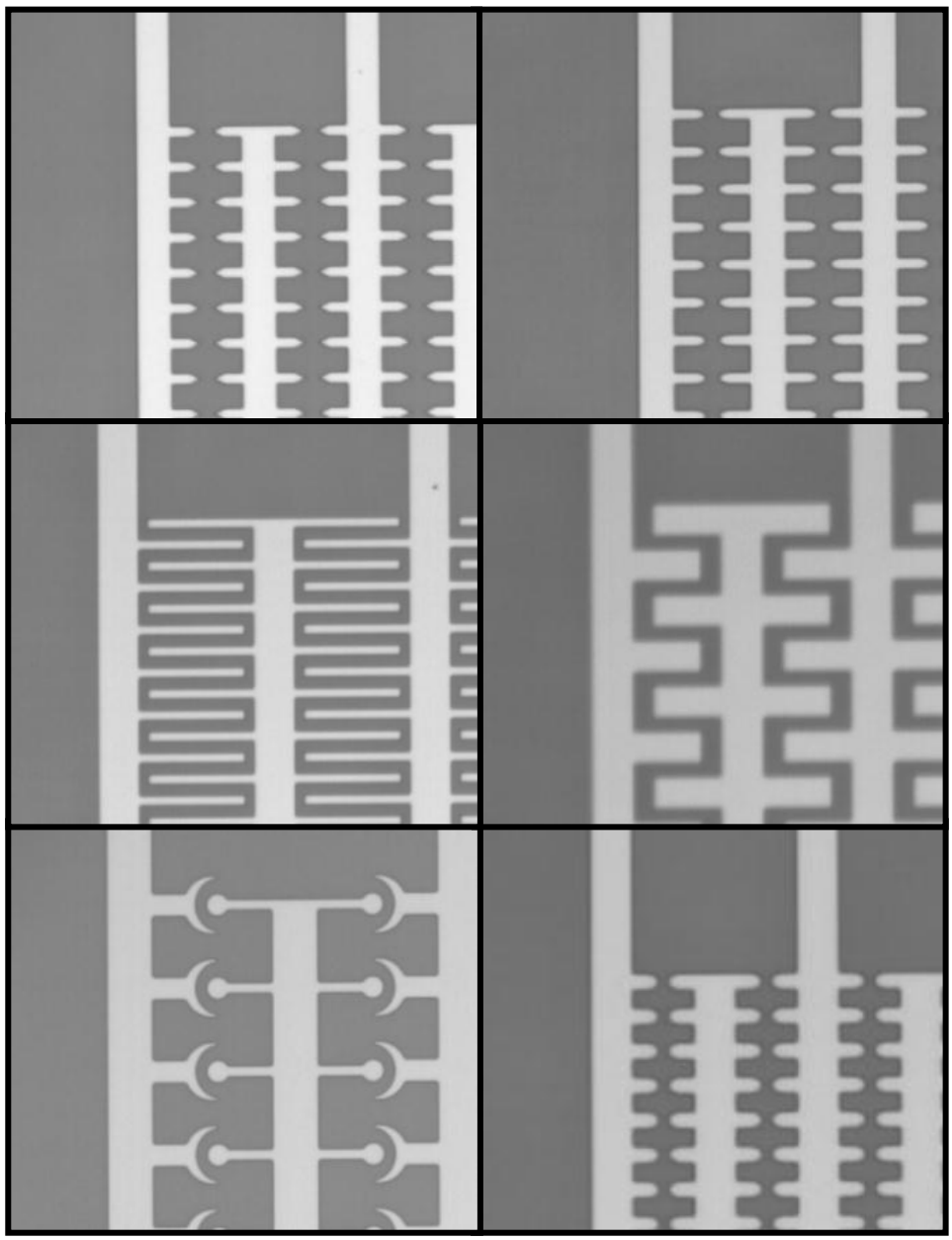

Figure 4.1 Some representative shapes of electrode array.

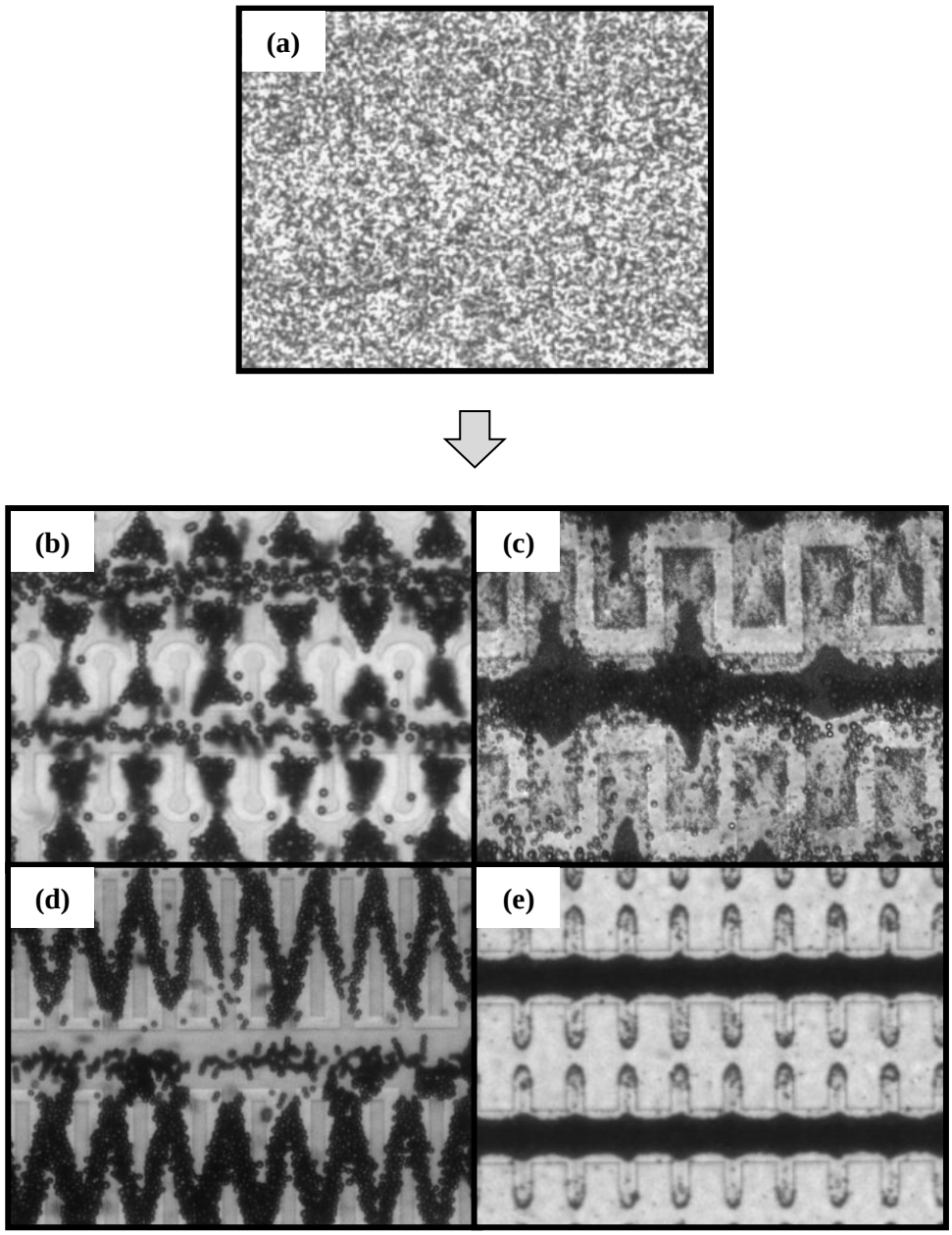

Figure 4.2 Experiments with microbeads. The photograph (a) before the voltage applied and after the voltage turned on. Beads were differently arranged by the distinct electrode arrays such as the shapes of (b) crescent, (c) crossed rectangles, (d) narrow crossed rectangles and (e) fingers.

4.2 The optimized electrode shape

Experiments with microbeads were conducted to predict magnitude of DEP force depending on electrode shape. We gradually increased the voltage from zero, and the frequency as well. As the input power had higher AC field, larger DEP force was derived. However if the voltage was higher than certain level, electrolysis was generated and then all electrodes were burned out. On the contrary, if the frequency was blow than tens of kHz at 5 V or more, electrolysis occurred as well.

Although DEP effectively worked like **Figure 4.2**, since ITO-glass wafer did not have pores, it was unable to measure drag force caused by viscous effect. Consequently, the selected shapes were fabricated on a silicon nitride wafer which contained pores and tested with beads again. Viscous effect made the results a bit different. After comparing the results, we chose two shapes which showed the highest efficiency; the results are as presented in **Figure 4.3**. We brought these decisions into experiments with real blood cells.

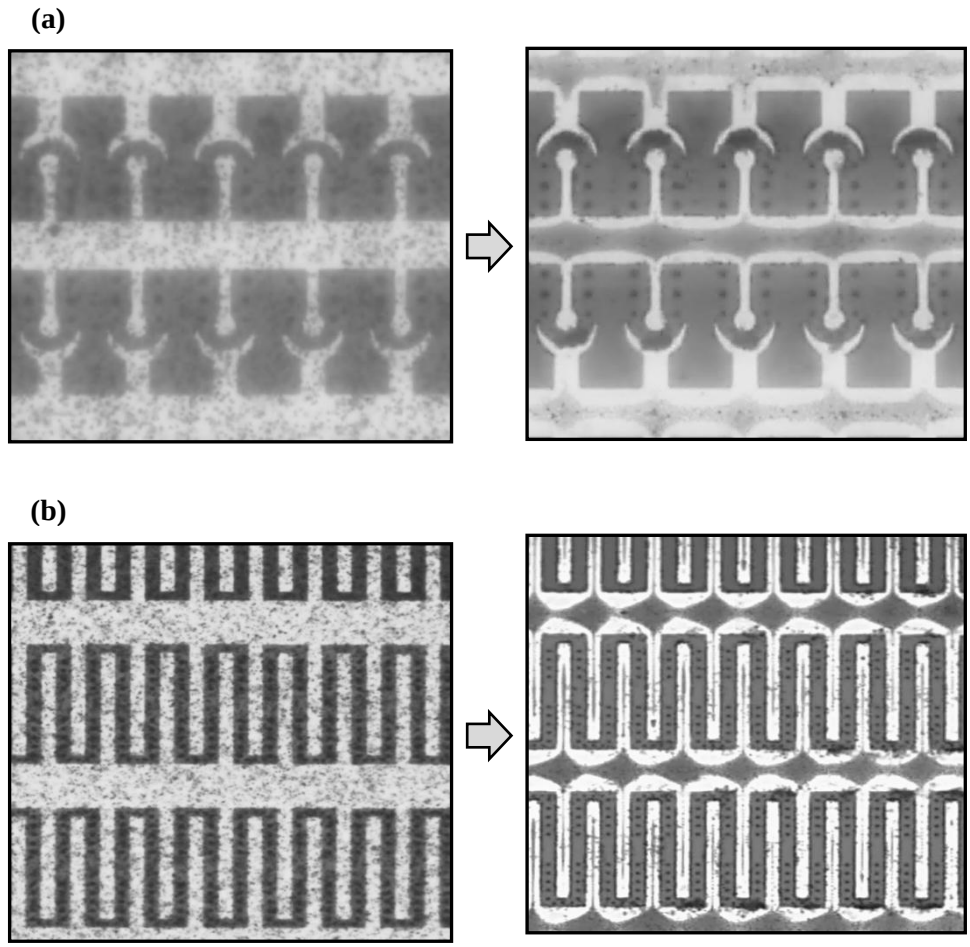

Figure 4.3 Two different electrode shapes which could generate strong DEP force. The areas which seem brighter are electrodes and the perfectly circular black dots between electrodes are micropores. The diameters of pore in both cases are 8 μm. It was unable to find pores in photos before DEP applied, nevertheless, pores came into view after beads were trapped onto electrodes.

4.3 Experiment with blood cells

4.3.1 Purity

Since viscosity of blood is even higher than that of bead solution, mobility of blood cells was remarkably decreased compared to microbeads. It led ambiguous boundary of cells distribution and left narrow pore array region because cells were less moved than we expected at first. Although two electrode shapes decided by pretest showed good performance, electrode in **Figure 4.4 (a)** was not able to be used practically, since there was not enough area to make pores in blood test as shown in **Figure 4.4 (a).** The small amount of pore area induced that plasma could not pass through the device easily. Therefore we selected crossed rectangular shape as the optimized one like **Figure 4.4 (b)**. We counted the number of red bold cells which remained in specified area noted by white solid line in **Figure 4.4,** and reported the ratios between with and without DEP. With same structure, we only modified dimensions of electrode, such as gap between electrodes and aspect ratio of them. After the voltage was applied (1 MHz, 6.5 Vpp), blood cells were repelled from electrode tip where the largest electric field exists, as shown in **Figure 4.5**. The most appropriate frequency for blood cells is about 1 MHz, a bit different from that for beads and this process was completed within 4 min. The concentration of blood mixture with isotonic buffer was 40:1.

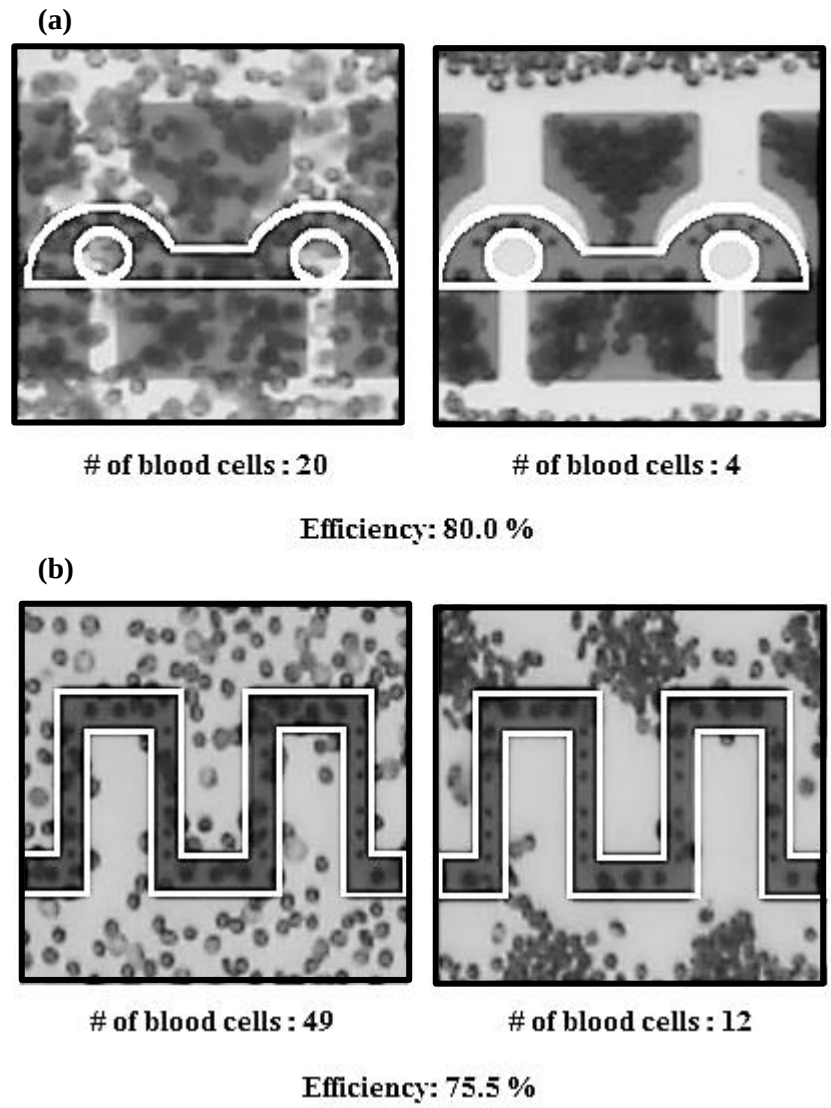

Figure 4.4 Cell removal efficiencies of two shapes. Left photos were taken before the voltage applied and right two photos were with DEP.

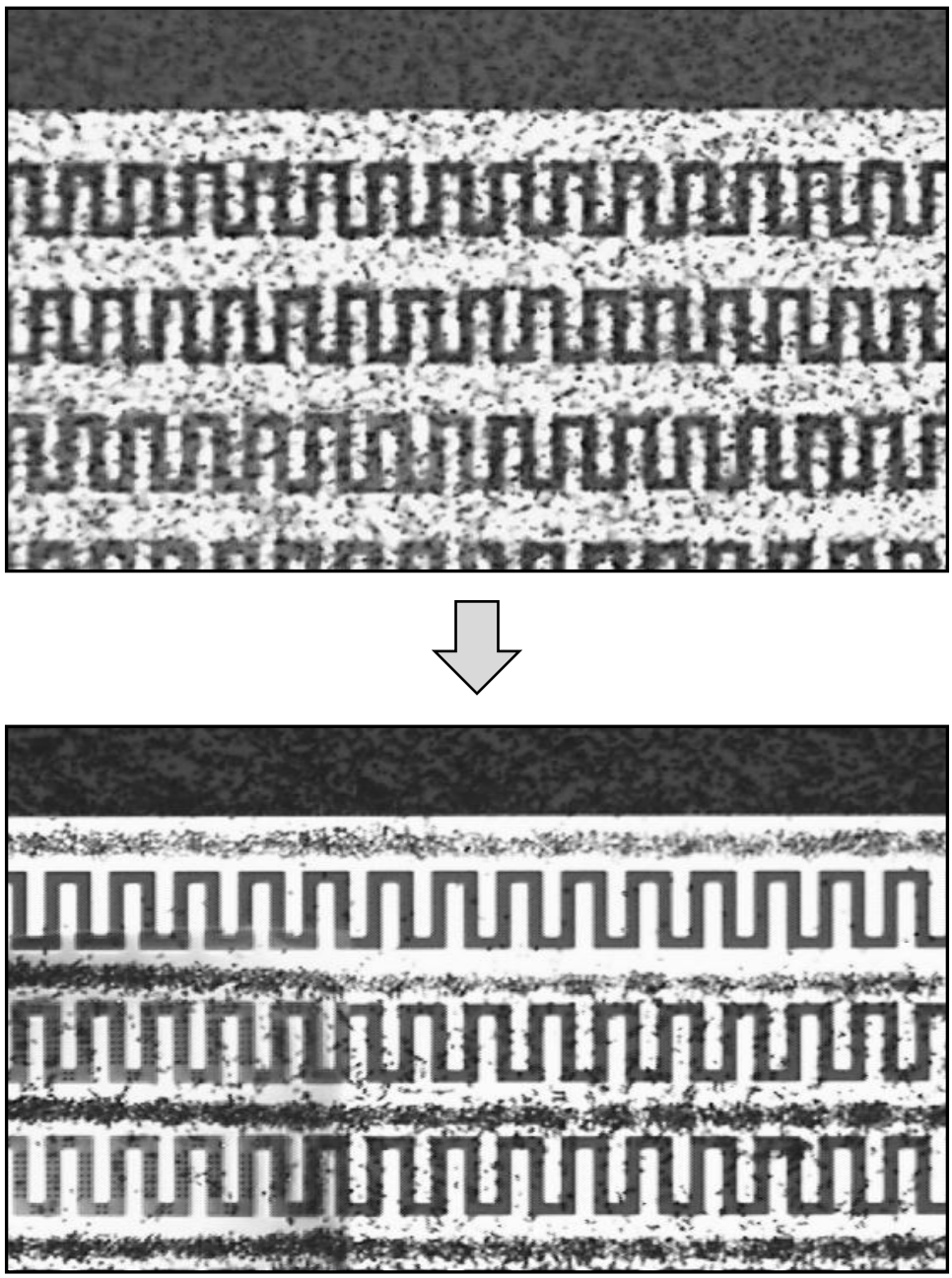

Figure 4.5 Pictures of diluted blood before/after voltage applied on the optimized device (Voltage: 6.5 Vpp, frequency: 1 MHz, time: < 4 min).

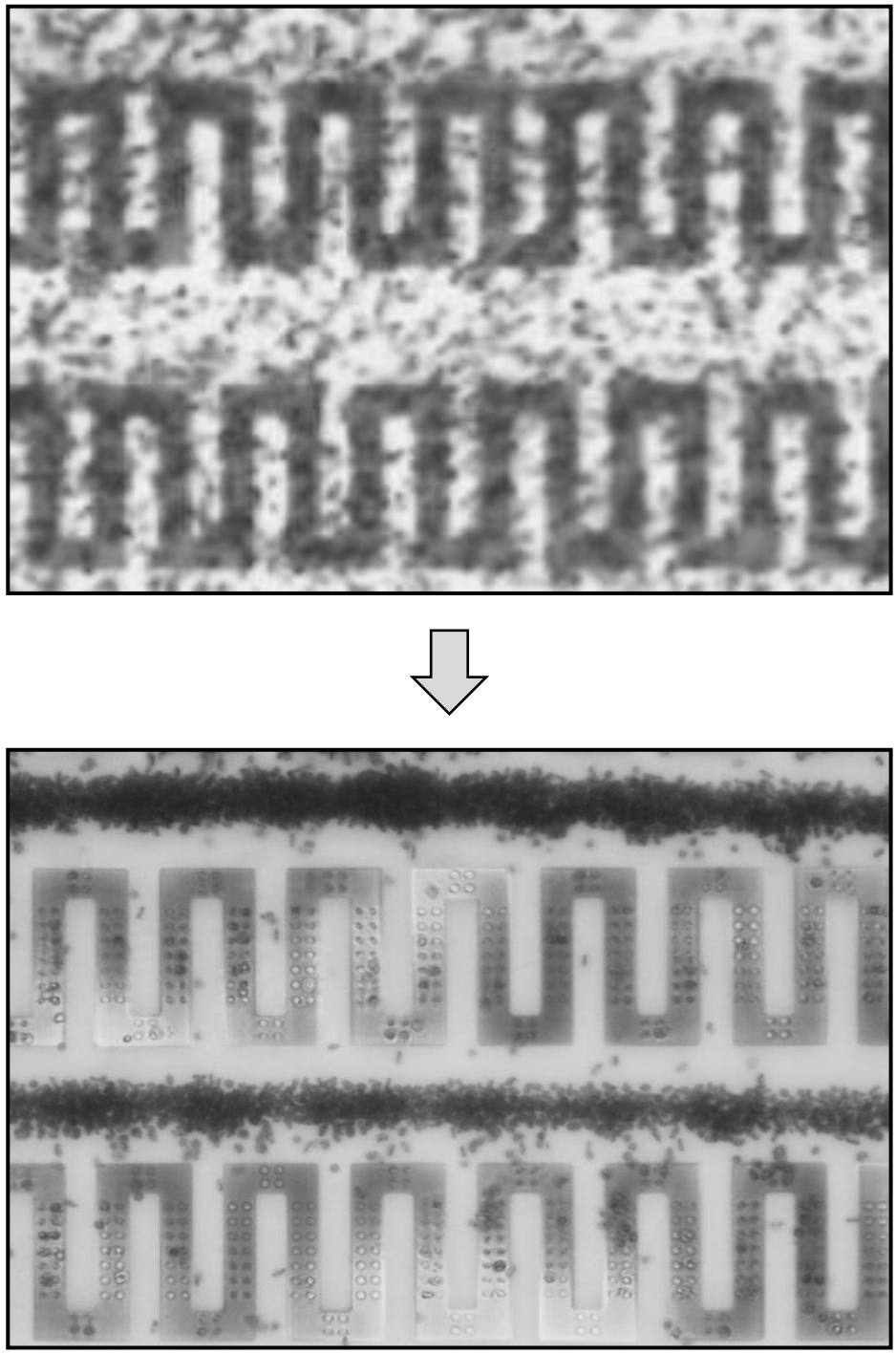

Figure 4.6 The magnified pictures of **Figure 4.5**. Circular figures between electrodes represent pores.

4.3.2 Recovery

The pore array, meanwhile, was tested with diluted blood. Although there have been an upper fluidic channel on the device, we did not use it while pore performance was tested. Blood sample was dropped right onto the region where pore and electrode arrays were, in order that we reported the numerical change in the contact angle. After measuring an initial contact angle, it was compared with another contact angle after certain minutes; we usually set the interval for 5 min. By using a contact angle and a radius of circular border plane between liquid and surface, it was possible to calculate the volume of the droplet. **Equation 4.1** and **Figure 4.7** explained the relationship.

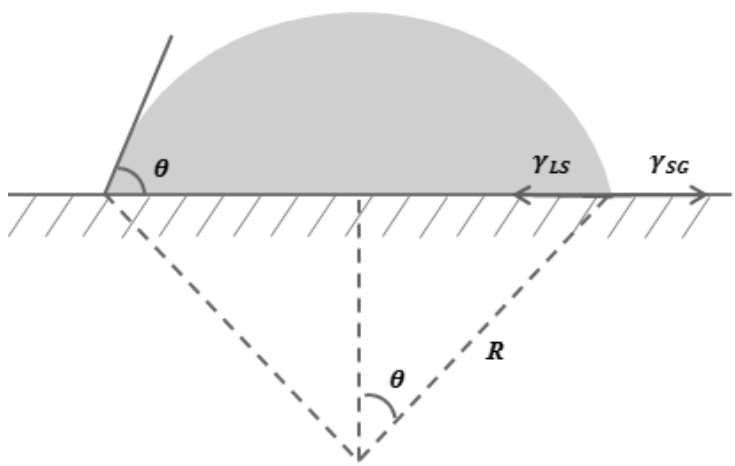

Figure 4.7 Schematic diagram of a droplet on surface.

$$\mathrm{V} = \frac{\pi R^3}{3}\,(1 - cos\theta)^2\,(2 + cos\theta) \qquad (\mathbf{4.1})$$

Capillary is the driving force, which let liquid above the device pass through the pores. However liquid could not be extracted well, because dimension of pores were very small. There was a trade-off between recovery rate and purity; if the pore widen, plasma flow goes up but cells also penetrate pores, hence purity decreases. Otherwise, the device has low recovery but high purity. Therefore, to determine a primary diameter range of pores was a very important step to make the optimized device. For this reason, we tested several devices which had different pore sizes.

To increase recovery rate, additional isotonic buffer was filled with the lower chamber and surface treatment was applied on the top and bottom side of the chip. The types of surface treatment were different according to region. A lower surface and side wall of pores should be hydrophilic so that filtered plasma could be easily diffused. The area around electrode arrays on an upper surface should also have hydrophilicity due to hydrophobicity of gold. The rest of the upper part, in contrast, hydrophobic treatment was required for making sessile drop with a high contact angle. Laplace pressure (Δp) in **Equation 4.2** tells that the higher contact angle droplet has, the larger pressure it generates.

$$\Delta p = \gamma \left(\frac{1}{R_1} + \frac{1}{R_2}\right) \qquad (\mathbf{4.2})$$

In case of R_1 being equal to R_2, equation could be

$$\Delta p = \gamma \frac{2}{R} \qquad (4.3)$$

where Δp is a pressure difference, γ is the surface tension and R is the radius of curvature of the droplet. **Figure 4.8** is a schematic diagram about surface treatment.

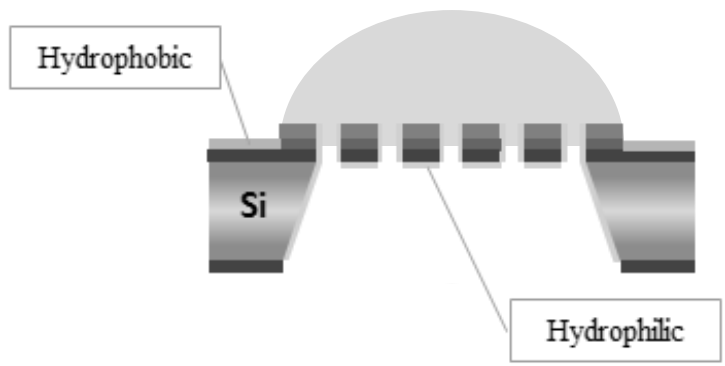

Figure 4.8 Concept about surface treatment and sessile drop.

It was confirmed that serum passed through the pore membrane and the height of serum droplet was slowly decreased. **Figure 4.9** shows the changes in contact angles 5 min after blood was dropped. The device with a diameter of 5 μm or more permitted all blood to pass through. On the other hand, blood stream was stopped with others.

(a)

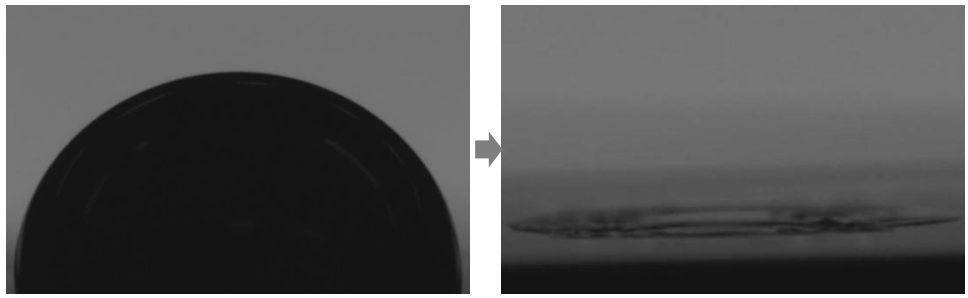

(b)

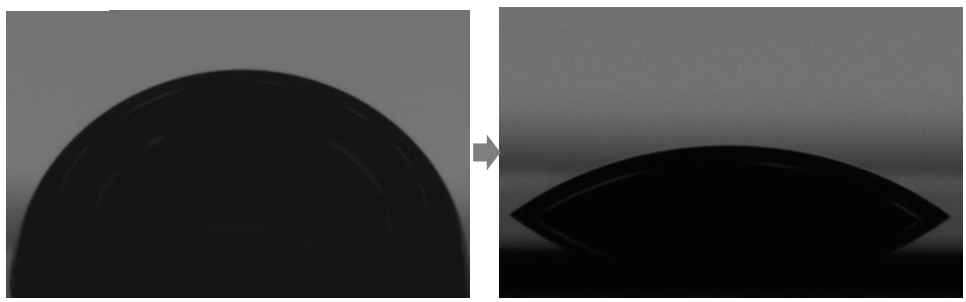

Figure 4.9 Shrinking droplets with (a) 5 **μm** pores and (b) 3 **μm** pores, 5 min after blood dropped on the surface. In the device with a diameter of 3 **μm**, Pores were blocked with blood cells and blood flow was stopped.

We measured recovery and purity depending on 5 different diameters of pores and results from them were plotted on a graph as shown in **Figure 4.10.** Purity was calculated by counting the number of red blood cells before and after filtration per unit area. If the pore size exceeded 9 μm, processes were rapidly finished. It meant DEP could not work because of strong drag force. By comparing between **Figure 4.11** (9 μm pores) and **Figure 4.12 (a)** (5 μm pores), it was easy to recognize that blood cells were not filtered by the device,

(a)

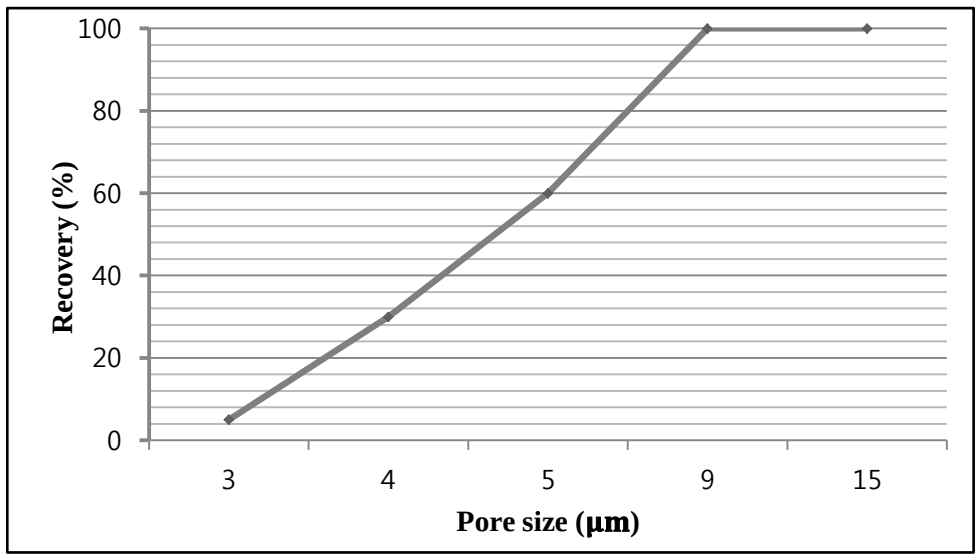

(b)

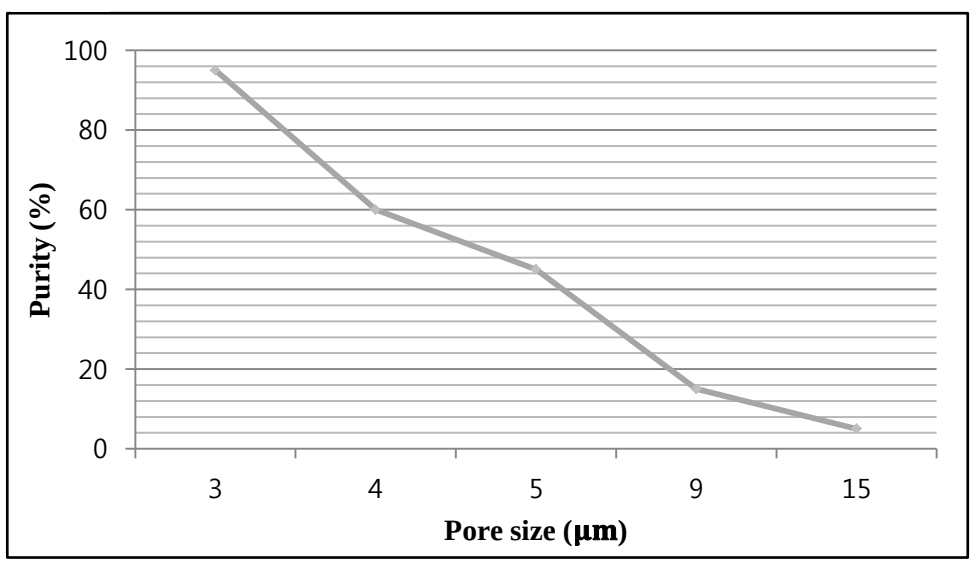

Figure 4.10 Two graph of (a) recovery and (b) purity with respect to pore size. Data were reported 3 min after process started to work.

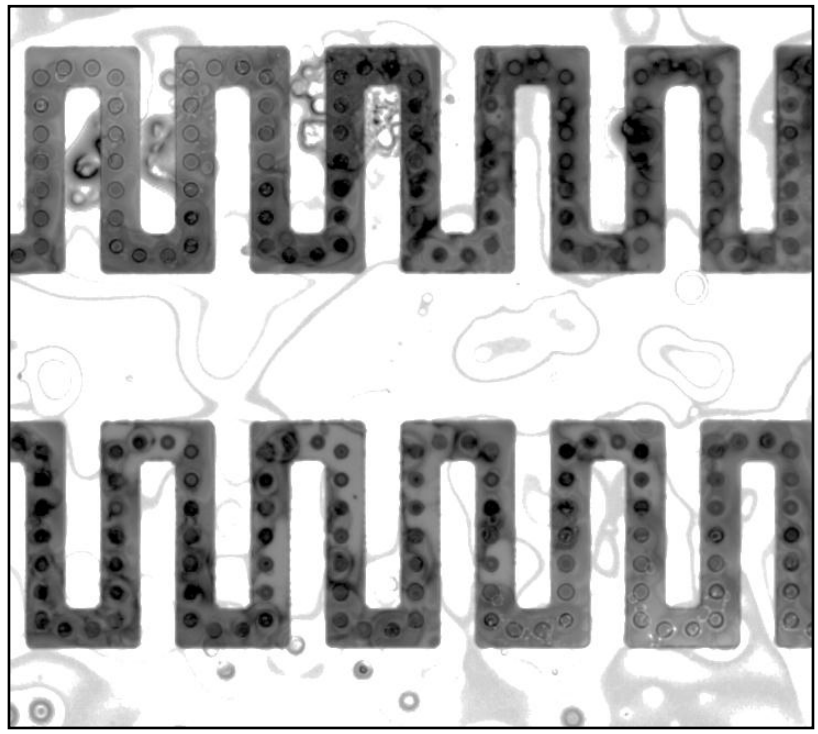

Figure 4.11 Top view of the device with 9 **μm** pore after separation process. Blood cells did not remain; they got swept away by the flow of liquid.

On the basis of the results, the proper pore size was able to be estimated. **Figure 4.10** gave us the optimized pore size and proper running time. Considering both recovery and purity of the device, pores with a diameter of 4 μm to 5 μm are suitable to assure high throughput separation. As can be seen **Figure 4.9,** 5 min was enough time to extract all plasma from the initial drop with the 5 μm pores. Here, though we did not use the upper fluidic channel to measure the accurate volume change, purity can be increased when the channel is installed.

4.3.3 DEP effectiveness

To figure out DEP effectiveness, we experimented with two same samples under same conditions but the only different thing was whether DEP was tuned on or not. **Figure 4.12 (a)** definitely shows the DEP effect. Red blood cells were stacked on electrodes, so pores were exposed; its pattern was similar with **Figure 4.6**. **Figure 4.12 (b)** was contrary to previous one. Without DEP, cells were randomly stuck onto the device. Since cells even blocked pores, plasma could not penetrate.

(a)

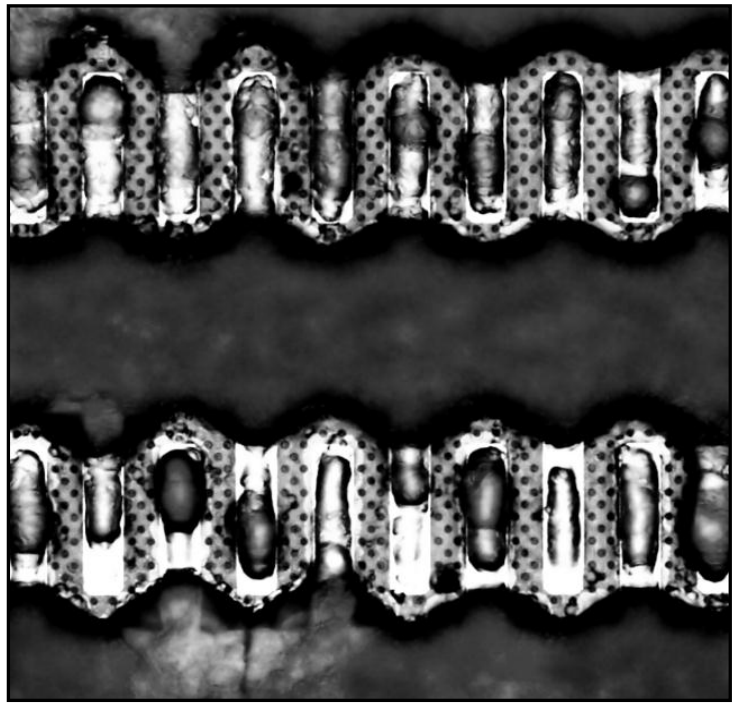

(b)

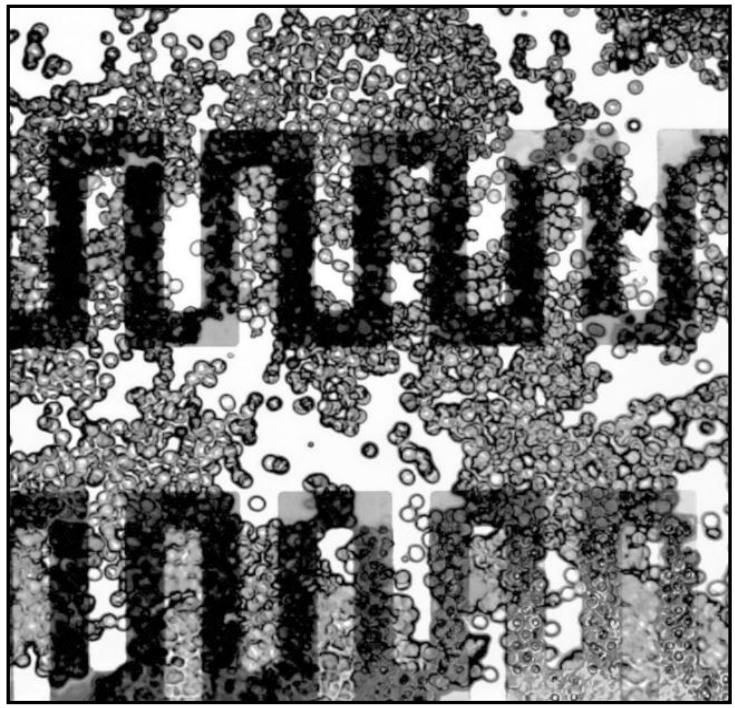

Figure 4.12 Filtration on the device with 5 **μm** pore. DEP was turned (a) on and (b) off.

5. Conclusion

We studied several techniques which is required for developing blood separation system. It has been an important part of the present diagnostic sensors. As DEP was one of the powerful tools for manipulating biological cells, it was demonstrated that liquid in mixture with particles was passed through pores without blocking effect while particles were repelled from pore array region by DEP. Using this technique, we succeeded in separating blood cells from plasma. It was able to be achieved with assistance from micropore array under hydrodynamic systems. We found the proper frequency and voltage (1 MHz, 6.5 Vpp each) when negative DEP were derived on blood cells. Moreover, the electrode array on our devices is the optimal shape in consequence of many pre-experiments. From the analyzed results, this device showed the fast processing time which means that it had high recovery rate. Especially by the device with diameter of 4 μm to 5 μm, process was over within 5 min, maintaining certain level of purity (more than 60%). We expected that blood plasma collected in the channel of this device can be used for various biological diagnostic sensors.

References

[1] Y. Nakashima, S. Hata, and T. Yasuda, “Blood plasma separation and extraction from a minute amount of blood using dielectrophoretic and capillary forces,” Sensors and Actuators B, 145, pp. 561-569, 2010.

[2] T. A. Crowley and V. Pizziconi, “Isolation of plasma from whole blood using planar microfilters for lab-on-a-chip applications,” Lab on a Chip, 5, pp. 922-929, 2005.

[3] D. Kim, J. Y. Yun, S. Park and S. S. Lee, “Effect of micro structure on blood cell clogging in blood separators based on capillary action,” Microsyst Technol, 15, pp. 227-233, 2009.

[4] I. K. Dimov, L. Basabe, J. L. Garcia, B. M. Ross, A. J. Ricco, and L. P. Lee, “Stand-alone self-powered integrated microfluidic blood analysis system (SIMBAS),” Lab on a Chip, 11, pp. 845-850, 2011.

[5] Y. kim, S. Kim, D. kim, S. Park, and J. Park, “Plasma extraction in a capillary-driven microfluidic device using surfactant-added poly(dimethlysiloxane),”Sensors and Actuators B, 145, pp. 861-868, 2010.

[6] S. Choi, T. Ku, S. Song, C. Choi and J. Park “Hydrophoretic high-throughput selection of platelets in physiological shear-stress range,” Lab on a Chip, 11, pp. 413-418, 2011.

[7] X. Chen, D. F. Cui, C. C. Liu and H. Li, “Microfluidic chip for blood cell separation and collection based on crossflow filtration,” Sensors and Actuators

B, 130, pp. 216-221, 2008.

[8] V. VanDelinder and A. Groisman, “Separation of plasma form whole human blood in a continuous cross-flow in a molded microfluidic device,” Anal. Chem, 78, pp. 3765-3771, 2006.

[9] Z. Geng, L. Zhang, Y. Ju, W. Wang, and Z. Li, “A plasma separation device based on centrifugal effect and Zweifach-Fung Effect,” 15th international Conference on Miniaturized Systems for Chemistry and Life Sciences 2011, Washington, pp.224-226.

[10] Z. Fekete, P. Nagy, G. Huszka, F. Tolner, A. Pongracz and P. Furjes “Performance characterization of micromachined particle separation system based on Zweifach-Fung effect,” Sensors and Actuators B, 162, pp. 89-94, 2012.

[11] A. Lenshof, C. Magnusson and T. Laurell, “Acoustofluidics 8: Applications of acoustophoresis in continuous flow microsystems,” Lab on a Chip, 12, pp. 1210-1223, 2012.

[12] F. Shen, H. Hwang, Y. K. Hahn, and J. Park, “Label-free cell separation using a tunable magnetophoretic repulsion force,” Anal. Chem, 84, pp. 3075-3081, 2012.

[13] Y. Nakashima, S. Hata, and T. Yasuda, “Blood plasma separation and extraction from a minute amount of blood using dielectrophoretic and capillary forces,” Sensors and Actuators B, 145, pp. 561-569, 2010.

[14] I. Doh, and Y. Cho, “A continuous cell separation chip using hydrodynamic dielectrophoresis (DEP) process,” Sensors and Actuators A, 121, pp. 59-65,

2005.

[15] G. H. Markx, M. S. Talary and R. Pethig, “Separation of viable and non-viable yeast using dielectrophoresis,” Journal of Biotechnology, 32, pp. 29-37, 1994.

[16] H. Moon, K. Kwon, S. Kim, H. Han, J. Sohn, S. Lee, and H. Jung, “Continuous separation of breast cancer cells from blood samples using multi-orifice flow fractionation (MOFF) and dielectophoresis (DEP),” Lab on a Chip, 11, pp. 1118-1125, 2011.

초 록

본 논문은 진단 센서의 한 부분을 이루는 마이크로유체역학 기반의 장치 위에서 유전영동과 마이크로포어 배열의 효과에 관한 내용을 다룬다. 최적화된 장치의 구조와 그것의 공정 과정 또한 소개되어있다. 실험의 효율성 증진을 위한 많은 시도가 이루어졌는데 이를테면 최대의 유전영동 힘을 이끌어내려는 것, 포어를 통해 액체를 추출해 내려는 것, 작동시간을 감소시키려는 것 등이었다.

유전영동과 마이크로포어 배열을 포함한 박막, 이 두 가지 주요 기술은 마이크로유체역학 플랫폼 위에서 독립적으로 그러나 동시에 작동되었다. 유전영동 힘을 발생시키기 위해, 불균일한 전기장을 유도하는 전극의 배열이 필요하였다. 장치 위에, 특히 전극이 존재하는 부분 주위에는 총 4 개의 박막이 있는데, 각 박막은 혈장을 아래방향으로 통과시킬 수 있는 수천 개의 마이크로포어를 포함한다. 이러한 전극과 포어 배열은 질화막(SiN)을 가진 실리콘 웨이퍼 위에 MEMS 공정 과정을 통하여 만들어진다. 본 공정과정은 사진식각공정, 활성화이온을 이용한 건식식각공정, 물리적 증착법, 수산화칼륨 용액을 이용한 습식식각공정 등을 포함한다. 여러 가지 샘플을 가지고 입자들의 운동을 테스트하여 최적화된 전극 형상이 결정되었으며, 포어의 효율을

향상시키기 위해서 박막 주변에 표면처리도 가해졌다. 또한 마이크로유체역학적 채널은 장치의 양면에 각각 부착되었다.

본 실험은 이론적 식을 기반으로 한 예측에 의해 진행되었다. 음의 유전영동에 의해 유도되는 세포의 움직임에 관한 보다 구체적인 경향성을 알아내기 위해 마이크로 사이즈의 비드를 이용한 실험이 선행되었다. 최종적으로 본 연구를 통하여, 유전영동을 위한 작은 전압만으로도 적은 양의 희석된 전혈로부터 혈장을 추출해낼 수 있다는 것에 관한 가능성이 확인되었다.

주요어: 혈장 추출, 혈액 분리, 유전영동, 마이크로포어 배열, 마이크로유체역학

학 번: 2011-22898

감사의 글

지난 2 년 간의 연구 과정을 이 작은 논문에 담았습니다. 부족한 제가 이렇게 한 편의 논문을 완성하기까지 감사해야 할 분들이 너무 많습니다. 그 분들께 이 자리를 빌려 감사의 인사를 드리고 싶습니다.

우선 이 자리에 제가 있기까지 저를 길러주신 부모님, 항상 저를 믿어주시고 지지하여 주셔서 감사합니다. 언제나 제 걱정을 아끼지 않으시는 조부모님 그리고 외조모님께도 진심으로 감사 드립니다. 물심양면으로 저를 챙겨주시며 응원해주신 숙부, 숙모와 이모부, 이모, 그리고 어느새 커서 힘들 때 위로가 되는 동생에게도 감사의 말을 전하고 싶습니다.

부족하고 아무것도 모르는 제가 연구 주제를 정하고 실험에 몰두할 수 있게 모든 여건을 만들어 주신 이정훈 지도교수님께 진심으로 감사 드립니다. 표현한 적 없었지만, 교수님의 조언들은 연구가 무엇인지 몰랐던 제게 연구의 방향을 잡아가고 실험하는 방법을 깨닫게 해주었습니다. 졸업을 하고 나서도 교수님께 배웠던 노력의 자세를 잊지 않고 살아가겠습니다. 가까이서 저를 다독이시고 격려해주시며 많은 것을 알려주신 차미선 교수님께도 깊은 감사를 표합니다. 제가 나태해지고 게을러져 있을 때에도 변함없이 믿고 지켜봐 주셔서 감사합니다.

2 년간 함께 지낸 연구실원들에게도 많은 것을 받은 것 같습니다. 연구실 동료들을 보면서 제가 여전히 부족하다는 것을 느꼈으며 또 그만큼 많이 배울 수 있었습니다. 정승원, 권용주 박사님을 비롯하여 홍주희, 김윤호, 최준규, 신재하, 이성준, 이수진, 정한영, 전은용, 최승열, 유창혁, 최요셉, 최정인, 박진혁, Neha Verma, Prashant Purwar, Jayanti Das 선배님들과 김성구, 백상웅, Changve Cheah 등 동기 및 후배들과 같은 연구실에서 생활할 수 있어서 좋았습니다. 돌이켜보면 제 대학원 생활은 훌륭한 동료들과 함께했기에 더 즐거웠던 것 같습니다. 항상 웃는 얼굴로 대해주신 박미희, 권혜림 선생님, 고맙습니다. 일일이 이곳에 다 열거할 수 없지만 감사했던 마음만큼은 항상

가슴에 간직하겠습니다. 졸업 후에도, NMSL 의 멤버로서 함께한 시간들은 잊지 못할 것 같습니다.

청정실 생활에 적응하며 즐겁게 공정장비연구생을 마칠 수 있게 도와 주셨던 반도체공동연구소의 최용윤 실장님 및 직원 분들께도 감사의 말씀을 드립니다.

여러 가지 이유로 힘들 때도 있었지만 항상 옆에서 위로가 되며 힘이 되었던 친구들이 있었습니다. 같이 기숙사 생활을 했던 박지수, 김도빈 등 주변의 모든 친구들에게도 고맙단 말을 전하고 싶습니다.

어느새 2013 년, 그리고 27 살이 되었습니다. 이제는 나이가 더해지는 사실도 무뎌지는 듯 합니다. 무한할 것 같았던 20 대도 얼마 남지 않았으며 그렇게 생각했던 때는 점점 멀어져만 갑니다. 풀리지 않던 물리 문제를 하루 종일 고민하며 풀어냈을 때의 희열과 순수함으로부턴 더욱 멀리 온 것 같습니다. 내 앞가림만 하면 되었던 그 시절과는 달리 이제 점점 선택과 책임이 늘어간다는 것을 깨닫는 찰나에 드디어 학교의 울타리를 벗어나 사회에 첫 발을 내딛습니다. 새해 세웠던 많은 다짐들이 숱하게 무너질 때의 낙담도 이제는 무덤덤하지만 그래도 한 가지는 배운 것 같습니다. 거짓 다짐으로 새로운 시작에 의미를 부여하는 것보다 기본적인 마음의 자세가 바뀌어야 한다는 것. 훌륭한 많은 사람들과 만나면서 저는 아직 모든 면에서 많이 부족하다는 것을 진심으로 깨달았습니다. 학위는 하나 늘어났지만 더욱 낮은 마음으로 살아 가겠습니다. 자신을 스스로 진리의 바다에서 조약돌을 줍고 있는 어린 아이의 비유했던 뉴턴의 겸손함을 닮고 싶습니다. 제가 혼자 할 수 있는 것은 아무 것도 없음을 고백하며 마지막으로, 저의 시작부터 끝까지 동행하시는 주님, 감사합니다.

Not because of who I am, but because of what you've done
Not because of what I've done, but because of who you are.

2013 년 1 월 31 일 목요일 밤.
연구실에서.